T.R.
ONDOKUZ MAYIS UNIVERSITY
INSTITUTE OF GRADUATE STUDIES
DEPARTMENT OF ANATOMY

MORPHOMETRIC ANALYSIS OF THE THIRD VENTRICLE AND CORPUS CALLOSUM IN MULTIPLE SCLEROSIS PATIENTS: MRI STUDY

Ph.D. Thesis

Hussam ALABDULLAH

Supervisor

Assoc. Prof. Dr. Mennan Ece PİRZİRENLİ

SAMSUN
2023

.ACCEPTANCE AND APPROVAL OF THE THESIS

The study entitled **"MORPHOMETRIC ANALYSIS OF THE THIRD VENTRICLE AND CORPUS CALLOSUM IN MULTIPLE SCLEROSIS PATIENTS: MRI STUDY"** prepared by **Hussam ALABDULLAH**, and supervised by **Assoc. Prof. Dr. Mennan Ece PIRZIRENLI** , was found successful and unanimously accepted by committee members as Ph.D. thesis, following the examination on the date 18.8.2023 .

	Title Name SURNAME **University** **Department/Art**	**Final Decision**
Chairman	Assoc. Prof. Dr. Mennan Ece PİRZİRENLİ Ondokuz Mayıs University Department of Medicine	☒ Accept ☐ Reject
Member	Prof. Dr. Aymen WARİLLE Ondokuz Mayıs University Department of Medicine	☒ Accept ☐ Reject
Member	Assoc. Prof. Dr. Aslı TANRIVERMİŞ SAYIT Ondokuz Mayıs University Department of Medicine	☒ Accept ☐ Reject
Member	Assoc. Prof. Dr.Zülal ÖNER Izmir Bakırçay University Department of Medicine	☒ Accept ☐ Reject
Member	Assist. Prof. Dr.Murat GÖLPINAR Hitit University Department of Medicine	☒ Accept ☐ Reject

This thesis has been approved by the committee members that already stated above and determined by the Institute Executive Board.

.

Prof. Dr. Ahmet TABAK
Head of Institute of Graduate Studies

DECLARATION OF COMPLIANCE WITH SCIENTIFIC ETHIC

I hereby declare and undertake that I complied with scientific ethics and academic rules in all stages of my Ph. D. Thesis , that I have referred to each quotation that I use directly or indirectly in the study and that the works I have used consist of those shown in the sources, that it was written in accordance with the institute writing guide and that the situations stated in the article 3, section 9 of the Regulation for TÜBİTAK Research and Publication Ethics Board were not violated.

Is Ethics Committee Necessary?

Yes ☒

No ☐

18 /08 / 2023
Hussam ALABDULLAH

DECLARATION OF THE THESIS STUDY ORIGINALITY REPORT

Thesis Title : MORPHOMETRIC ANALYSIS OF THE THIRD VENTRICLE AND CORPUS CALLOSUM IN MULTIPLE SCLEROSIS PATIENTS: MRI STUDY

As a result of the originality report taken by me from the plagiarism detection program on 20 /06 /2023 for the thesis titled above;

Similarity ratio : % 14

Single resource rate : % 1 has been released.

18 /08 / 2023
Assoc. Prof. Dr. Mennan Ece PİRZİRENLİ

ÖZET

MULTİPLE SKLEROZ HASTALARINDA ÜÇÜNCÜ VENTRİKÜL VE CORPUS CALLOSUM ANATOMİSİNİN MORFOMETRİK ANALİZİ: MANYETİK REZONANS GÖRÜNTÜLEME ÇALIŞMASI,

Hussam ALABDULLAH
Ondokuz Mayıs Üniversitesi
Lisansüstü Eğitim Enstitüsü
ANATOMİ ANA BİLİM DALI
Doktora, Ağustos/2023
Danışman: Doç. Dr. Mennan Ece PİRZİRENLİ

Üçüncü ventrikül (3V) genişlemesi ve Corpus callosum (CC) atrofisi, (MS) hastalarında merkezi beyin atrofisini belirlemede nesnel bir gösterge olarak önerilmiştir. MS ile ilgili beyin atrofisi araştırmalarındaki artan ilgiye rağmen, çoğu çalışma 3V ve CC 'nin birkaç anatomi parametresine odaklanmıştır. Daha kapsamlı bir değerlendirme için, bu çalışma, kolay lineer MRI ölçümlerini kullanarak MS hastalarında 3V ve CC 'nin anatomik değişikliklerini ele almayı ve sonuçları normal populasyonla karşılaştırmayı amaçlamaktadır.

OMÜ öğretim hastanesinden 2017-2021 yılları arasında gerçekleştirilen 50 beyin MRI taraması (25 MS hastası ve 25 sağlıklı kontrol) seçildi. Yaşları 23 ile 48 arasında olan bireyler dahil edildi. 3V 'nin beş parametresi ve CC 'nin beş parametresi değerlendirildi.

Sonuçlar, hastaların ortalama üçüncü ventrikül genişliğinin (W1) ventrikülün maksimum uzun ekseninin orta noktasında axial düzlemde ölçülen 6,08±2,34 mm, kontrollere kıyasla 2,67±0,63 mm (p=0,00) anlamlı derecede daha geniş olduğunu gösterdi. Aynı durum, hastaların interventriküler foramen seviyesinde ölçülen ortalama üçüncü ventrikül genişliği (W2) için de geçerlidir ve bu ölçümde hastaların genişliği 6,64±1,85 mm, kontrollerin ise 3,66±0,64 mm (p=0,00) olarak anlamlı derecede daha geniştir. Ventrikülün yüksekliği (H) (p=0,21) ve uzunluğu (L) (p=0,6) açısından önemsiz farklar tespit edildi. CC parametreleri açısından yapılan t-testi sonuçları, iki grup arasında genu (G) (p=0,000), body (B) (p=0,000), splenium (S) (p=0,000), anteroposterior çapı (AP) (p=0,008) ve corpus callosum indeksi (CCI) (p=0,000) için istatistiksel olarak anlamlı bir fark olduğunu ortaya koymuştur.

Sonuç olarak, dikkat çeken bulgu, ölçüm seviyesinden bağımsız olarak üçüncü ventrikülün genişlemesidir. MS hastaları, nörolojik olarak normal kişilere kıyasla anlamlı derecede daha ince CC segmentlere sahiptir.

Anahtar Sözcükler: Üçüncü ventrikül, Corpus callosum, Multipl skleroz, MRG, Beyin atrofisi.

ABSTRACT

MORPHOMETRIC ANALYSIS OF THE THIRD VENTRICLE AND CORPUS CALLOSUM IN MULTIPLE SCLEROSIS PATIENTS: MRI STUDY

Hussam ALABDULLAH
Ondokuz Mayıs University
Institute of Graduate Studies
Department of Anatomy
Ph.D., August/2023
Supervisor: Assoc. Prof. Dr. Mennan Ece PİRZİRENLİ

The third ventricle (3V) enlargement and corpus callosum (CC) atrophy have been proposed as subjective indicators for identifying central brain atrophy in multiple sclerosis (MS) patients. In spite of the increasing interest in MS-related brain atrophy research, most studies have tended to focus on a few anatomic parameters of the 3V and CC. For a more comprehensive evaluation, this study aims to address the anatomical changes of the 3V and CC in MS patients using easy linear MRI measurements and compare the results with those in the normal population.

Fifty brain MRI scans (25 MS patients and 25 healthy controls) performed between 2017 and 2021 were selected from OMU Medical Faculty hospital. Individuals aged between 23 and 48 years. In this study five parameters of the 3V and five parameters of the CC were determined and evaluated.

Results demonstrated that patients' mean third ventricular width (W1) measured in the axial plane at the midpoint of the maximum long axis of the ventricle 6.08±2.34 mm was significantly wider compared to controls 2.67±0.63 mm ($p = 0.001$). The same is true for patients' mean third ventricle width (W2) measured at the level of the interventricular foramen 6.64±1.85 mm, which was also significantly wider compared to controls 3.66±0.64 mm ($p = 0.00$). An insignificant difference regarding the height of the ventricle (H) with ($p = 0.21$) and length (L) with ($p = 0.6$) was noticed. As for the CC parameters, the results of the t-test revealed that there is a statistically significant difference between the two groups for genu G ($P = 0.000$), body B ($P = 0.000$), splenium S ($P = 0.000$), anteroposterior diameter AP ($P = 0.008$), and corpus callosum index (CCI) ($P = 0.000$).

In conclusion, the noteworthy finding was the widening of the third ventricle, regardless of the level of measurement. MS patients had significantly thinner CC segments than their neurologically normal counterparts.

Keywords: Third ventricle, Corpus callosum, Multiple sclerosis, MRI, Brain atrophy.

ACKNOWLEDGEMENT

I would like to express my deepest gratitude to my Supervisor: Assoc. Prof. Dr. Mennan Ece PİRZİRENLİ for her invaluable patience and feedback, who generously provided knowledge and expertise. Additionally, this endeavor would not have been possible without the generous support and academic guidance from Assoc. Prof. Dr. Aslı Tanrıvermiş Sayıt and Prof. Dr. Aymen Warille.

I would like also to extend my sincere thanks to all the professors and colleagues in the anatomy, radiology, and statistics departments for their assistance and inspiration.

Lastly, I would be remiss in not mentioning my family, especially my lovely wife and children. Their belief in me has kept my spirits and motivation high during this journey.

Hussam ALABDULLAH

CONTENTS

SYMBOLS AND ABBREVIATIONS

2D	: two-dimensional
3V	: Third Ventricle
A.D.	: Anno Domini . It refers to the birth of Jesus Christ
AC	: Anterior Commissure
ACT	: Adrenocorticotropic Hormone
AP	: Anteroposterior Diameter
ALV	: Ascending Lumbar Vein
B	: Body
B.C.	: Before Christ
CC	: Corpus Callosum
CCI	: Corpus Callosum Index
CCV	: Corpus Callosum Volume
CIS	: Clinically Isolated Syndrome
CNS	: Central Nervous System
CSF	: Cerebrospinal Fluid
CT scan	: Computed Tomography Scan
DICOM	: Digital Imaging and Communications in Medicine
DIS	: Dissemination In Space
DIT	: Dissemination In Time
DMTs	: Disease-modifying Therapies
EBV	: Epstein-Barr Virus
EDSS	: Expanded Disability Status Scale
F:M Ratio	: Female: Male Ratio
G	: Genu
Gd	: Gadolinium
H	: Height of the Third Ventricle
L	: Length of the Third Ventricle
MRI	: Magnetic Resonance Imaging
MS	: Multiple Sclerosis
PC	: Posterior Commissure
PPMS	: Primary Progressive Multiple Sclerosis Vein

RRMS	: Relapsing-remitting Multiple Sclerosis
S	: Splenium
SPMS	: Secondary Progressive Multiple Sclerosis
SPSS	: Statistical Package For The Social Sciences
TCS	: Transcranial Sonography
TD	: Transverse Diameter of the skull
TVR	: Third Ventricle Ratio
UVB	: Ultraviolet B light
W1	: Width of the third ventricle at the midpoint of the length
W2	: Width of the third ventricle at the level of interventricular foramen

FIGURES LEGENDS

TABLES LEGENDS

1. INTRODUCTION

Multiple sclerosis (MS) is a chronic autoimmune disease that affects the central nervous system (CNS). It is a condition characterized by persistent inflammation and neurodegeneration within the nervous system. MS is a leading cause of neurological dysfunction among young individuals and comes after trauma (Dobson & Giovannoni, 2019). MS cases that are newly identified, are rising in all countries and affecting global economics (Browne et al., 2014). It is a complicated disease, and its exact etiology remains undisclosed.

Brain atrophy starts extremely early during the progressive stages of the disease, and affects not only the white matter but also the gray matter (Ghione et al., 2019). Atrophy is primarily unrelated to noticeable lesions (Fisniku et al., 2008) and develops at a rate that might be up to five times faster than normal aging (Miller et al., 2002). The causes of MS-related brain atrophy are the demyelination and axonal transection (Amiri et al., 2018). Furthermore, tissue loss caused by inflammation and demyelination may be somewhat reversible in relapsing-remitting MS (RRMS) (Filippi and Rocca, 2011), whereas other mechanisms of tissue loss may lead to irreversible axonal damage, particularly in progressive disease (Andravizou et al., 2019).

Assessing the loss of tissue in the CNS is attracting considerable interest, as it indicates the net effect of all pathological mechanisms that cause tissue destruction throughout the disease (Ghione et al., 2018). Central atrophy implies the loss of brain parenchymal volume, subsequently, there is a rise in the magnitude of spaces for cerebrospinal fluid (CSF), which is also visibly evident in the enlargement of ventricular system (Lutz et al., 2017). The expansion of ventricles in MS has been frequently researched, ranging from a comprehensive assessment of the total amount of CSF spaces to specific localized measurements of the third or fourth ventricle (Laffon et al., 2014). The third ventricle (3V) is a tiny hollow cavity in the middle of the diencephalon. Atrophy of nearby tissues, particularly the thalami, leads to an enlargement of the third ventricle. It has been demonstrated that people with MS have a larger third ventricle (Cifelli et al., 2002).

On the other hand, the corpus callosum (CC) is the brain's major fiber tract, connecting the two hemispheres (Gazzaniga, 2000). In the majority of cases with MS, CC is abnormal (Evangelou et al., 2000), owing to the fact that CC is engaged in

important tasks including cognition and sensory integration (Larson et al., 2002).

The utilization of magnetic resonance imaging (MRI) is prevalent in MS examinations as a diagnostic imaging modality. While MS continues to be diagnosed clinically, the utilization of MRI has proven to be an indispensable method for comprehending and tracking the disease, and is frequently employed to verify the diagnosis (Miller et al., 1998).

This study was designed to analyze in depth the structural alterations of the 3V and the CC among patients with MS, and aimed also to compare these findings with those of normal individuals.

2. GENERAL INFORMATION AND LITERATURE REVIEW

2.1. The Third Ventricle

2.1.1. Brief History of the Ventricular System

Erasistratus (304 BC - 250 BC) and Herophilus (335 BC - 280 BC), two Greeks who were permitted to do dissections on humans, may have written the earliest descriptions of human ventricular system in the third century BC (Mortazavi et al., 2014). Galen (129–217 AD) suggested that the ventricles seemed to be important for holding the animal soul. Galen noted that damage to the ventricles caused by trauma never resulted in death, despite the fact that sensation and movement were impaired (Dezena et al., 2020). Leonardo da Vinci, lived from 1452 to 1519. He was a pivotal figure in the development and essence of the Renaissance era, as seen by his improved depictions of the brain's ventricular system (Dezena et al., 2020). The father of contemporary anatomy refers to Andreas Vesalius (1514-1564), outstanding gross anatomical information on the ventricles was found in his anatomy book (Mortazavi et al., 2014). Despite the detailed accounts of the Renaissance, it was unclear if the ventricular cavities contained fluid or gas untill 1764, when an Italian scientist, Domenico Felice Antonio Cotugno found the answer to this mystery when he identified cerebrospinal fluid (Schiller, 1997). Foramen de Magendie, also known as the median aperture of the fourth ventricle, was discovered by French neurologist François Jean Magendie 1783-1855 (Tubbs et al., 2008). The lateral openings of the fourth ventricle were discovered in 1855 by a German anatomist named Hubert von Luschka (Schiller, 1997).

2.1.2. Histology of the Ventricular System

Ependymocytes are specialized cells, Lining the brain's ventricles, these cells are columnar cells or cuboidal cells developed from neuroepithelium. Just beneath the ependymal epithelium is the choroidal plexus, which is in charge of CSF secretion. There are two main types of ependymal cells seen in lateral ventricles: ciliated cells and nonciliated cells (Bruni et al., 1985). Subependymal glial cells reside under the ependymal layer, where the ependymal detailed integrated with surrounding astrocyte processes and blood vessels, helping to formulate blood-brain barrier (Gabrion et al., 1998). On the other hand, the ventricular system as a whole does not always have this barrier. The barrier is either weak or nonexistent along some of the third and fourth ventricles, allowing a nearly unrestricted flow of blood to and from these regions. The

pineal body and the median eminence are two examples of the structures that make up the group of structures known as the circumventricular organs (Figure 2.1) (Gabrion et al., 1998).

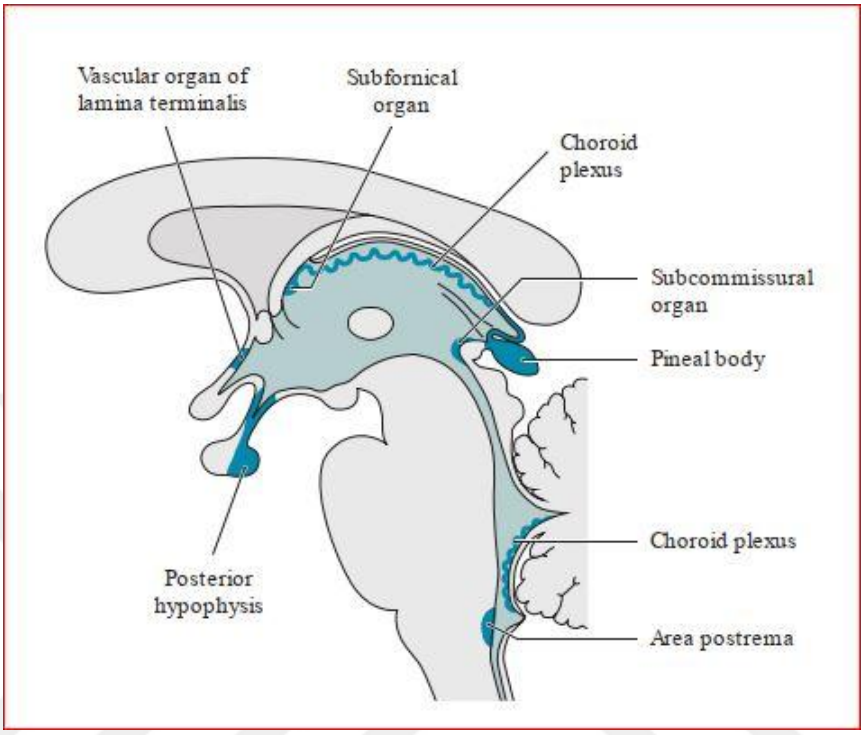

Figure 2.1. Circumventricular organs (Schuenke, 2016).

2.1.3. Embryology of the Ventricular System

Three dilatations appear in the cephalic region of the neural tube after occlusion. These three structures are called the prosencephalon, mesencephalon, and rhombencephalon, in a cephalocaudal direction. The telencephalon and diencephalon originate from the prosencephalon during the fifth week of gestation. Rhombencephalon serves as the precursor to both metencephalon, which encompasses the cerebellum and pons, and myelencephalon, also known as the medulla oblongata. (Figure 2.2) (Korzh, 2018).

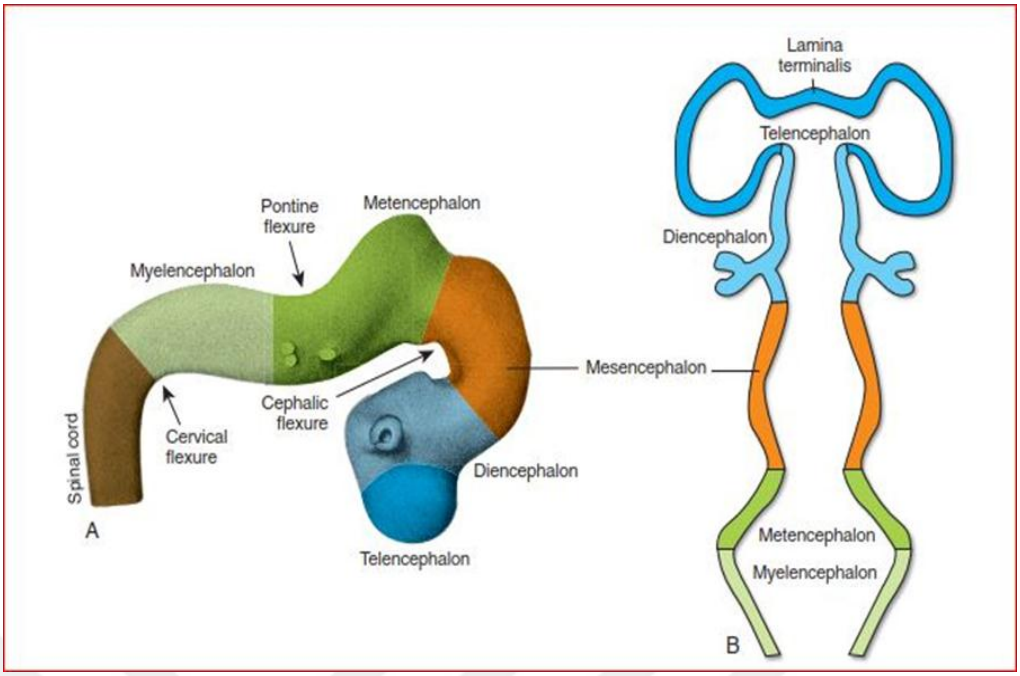

Figure 2. 2. Developement of neural tube and ventricular system (Vanderah, 2016)

These vesicles continue to have cavities within them, which will eventually become ventricles, and allow them to communicate with the interior of the neural tube. The lateral ventricles are positioned in telencephalon, third ventricle resides in the diencephalon, and the fourth ventricle lies in the rhombencephalon. The cerebral aqueduct is the lately narrowed cavity of the mesencephalon, which links both ventricles; third and fourth (figure 2.3) (Korzh, 2018).

2.1.4. Circulation of the CSF

The choroid plexus, which is located to a certain extent in each of the four cerebral ventricles, is the location where cerebrospinal fluid is released. It flows via the median aperture as well as the paired lateral apertures into the subarachnoid region, which includes enlargements that are named cisterns (Khasawneh et al., 2018). The cerebrospinal fluid (CSF) located in the subarachnoid space is gradually reabsorbed through the arachnoid granulations that are located in the superior sagittal sinus. Through a pressure-dependent gradient, cerebrospinal fluid (CSF) can be reabsorbed into the circulatory system through arachnoid granulations, which function as a conduit for this process. Arachnoid granulations protrude into the superior sagittal sinus due to a pressure gradient between the subarachnoid space and the venous sinuses, with the former exhibiting higher pressure levels (Khasawneh et al., 2018).

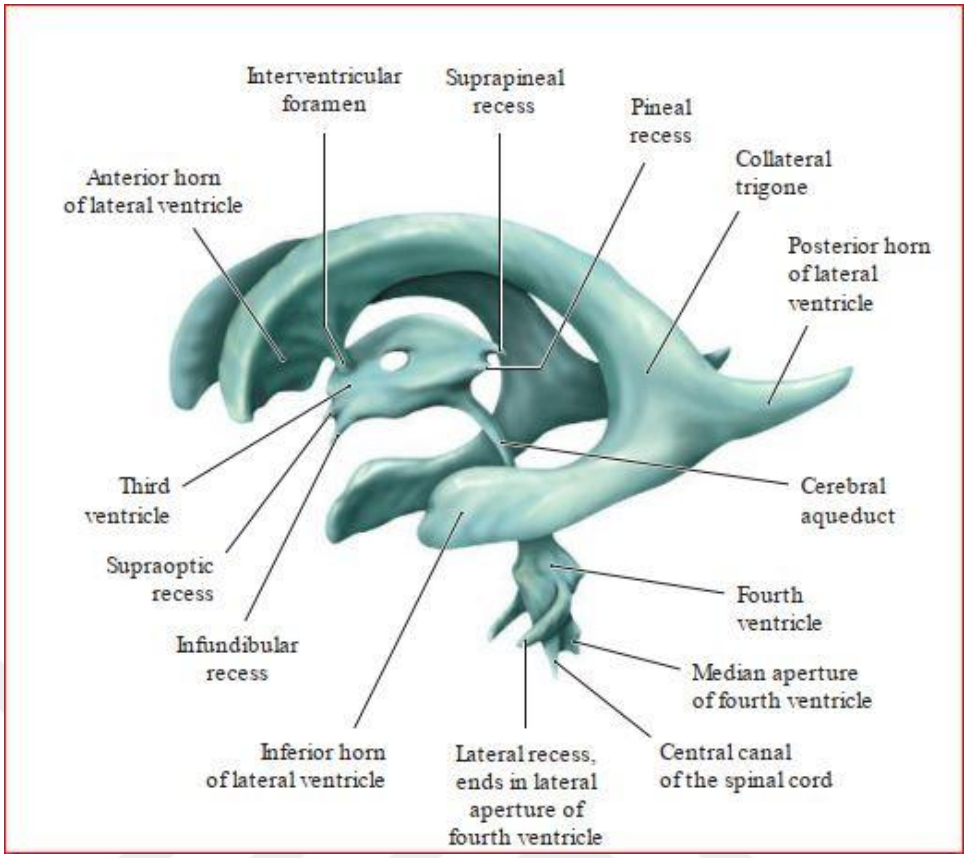

Figure 2.3. Brain ventricles (Schuenke, 2016)

2.1.5. Third Ventricle Anatomy

The third ventricle 3V sits in the middle of the cranium between cerebral hemispheres, just superior to the sella turcica and midbrain. It has closer relations to the Willis circle and its ramifications, as well as the Galen's great vien . Tumors in the third ventricle region are exceptionally challenging to diagnose and operate on due to their difficult anatomical position.

It is a thin, unilocular cavity that is connected through the foramen of Monro to the lateral ventricles, while the Sylvius aqueduct at its posterior margin connects it to the fourth ventricle. For anatomical description, it is bounded by a roof, floor, anteriorwall, and posterior wall with two lateral walls (Dezena et al., 2020).

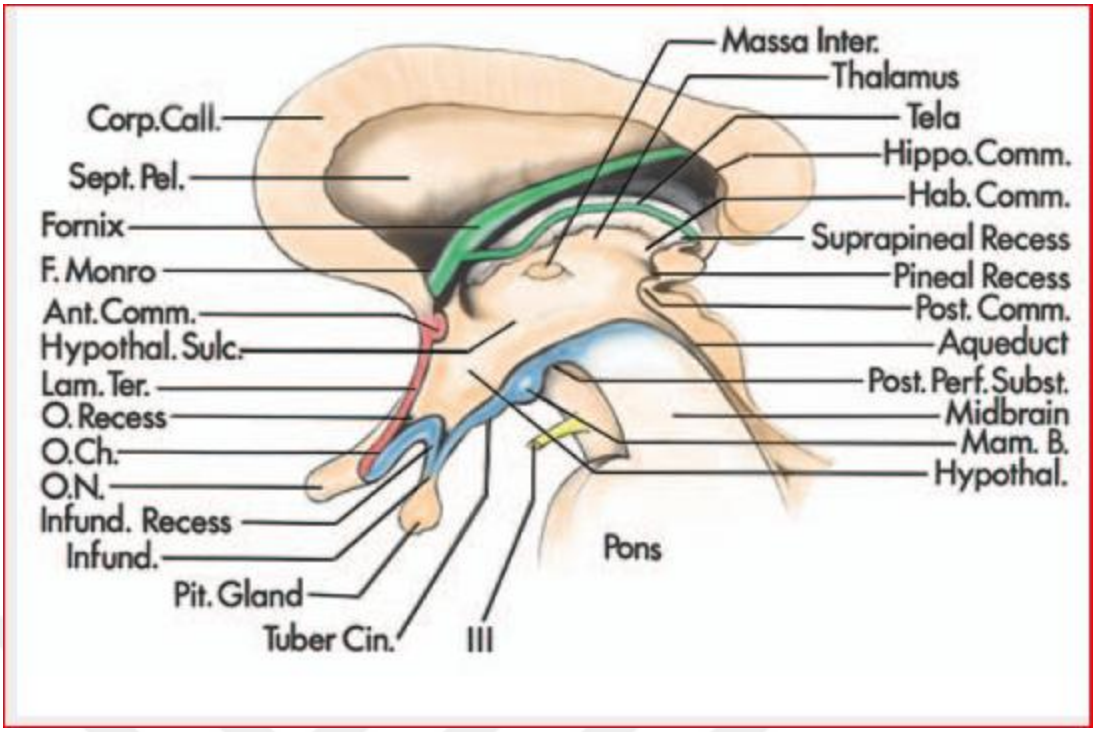

Figure 2. 4. The third ventricle (Rhoton, 2007)

2.1.5.1 Roof of the Third Ventricle

From Monro foramen in front to the suprapineal recess in the back, the roof of the ventricle creates a soft, upward curve. The roof is made up of four distinct layers: the fornix, which is made up of neural tissue, the two tela choroidea membranous layers encircling an intermediate vascular layer amidst them. In the roof's lateral edge, the choroidal fissure is located. The fornix crura and hippocampal commissure make up the posterior portion of the roof, whereas the body of fornix comprises the anterior portion. Septum pellucidum is connected to the fornix at its highest body surface (Tsutsumi et al., 2018).

The tela choroidea consists of a pair of slender, partially translucent membranes that arise from the pia mater and are connected by inadequately organized trabeculae. Medial posterior choroidal arteries make up the vascular layer, and tributaries of internal cerebral veins are also considered a part of this layer. In the upper region of the 3V, the parallel choroid plexus extends down on both sides of the midline (Tsutsumi et al., 2018).

The region of space that exists between both sheets of tela choroidea and makes up ceiling of the 3V is known as the velum interpositum (Zohdi & Elkheshin, 2012).

The suprapineal recess is a part of the 3V roof that sits superior to the pineal

body and below the tela choroidea. It's rare for the velum interpositum to have an opening bounded by splenium and pineal body that connects to the quadrigeminal cistern, but this is possible because the velum interpositum is generally closed and fades to a small apex beyond the interventricular foramen (Zohdi & Elkheshin, 2012).

2.1.5.2. Floor of the Ventricle

From the optic chiasm in the front to the cerebral aqueduct of Sylvius in the back, that's how long the floor is. Structures in the diencephalon make up the front half of the floor, while structures in the midbrain make up the back half. When inferiorly viewed, the floor is made up of the optic chiasm in front, then the infundibulum, then the tuber cinereum and the mamillary bodies, then the posterior perforated substance, and more caudally, there is the portion of the tegmentum of the mesencephalon situated medially above the cerebral peduncles (Fernandes-Silva et al., 2021).

The chiasm exhibits a posterior and superior inclination as it emerges from its convergence with the optic nerves. The front of the floor is formed by the inferior face of the chiasm, while the lower portion of the anterior wall is formed by the superior face of the chiasm (Fernandes-Silva et al., 2021).

The infundibulum is a hollow structure that takes the shape of a funneland is found between optic chiasm anteriorly and tuber cinereum posteriorly. The hypophysis, or pituitary gland, is connected to the infundibulum, and infundibulum fibers continue to posterior part of pituitary gland (Aydin et al., 2009).

Tuber cinereum, which is a significant area of gray matter in the hypothalamus, sits in front of mammillary bodies. Anteriorly, the tuber cinereum joins the infundibulum. Tuber cinereum at the infundibulum's base is elevated to produce a protrusion known as the median eminence (Aydin et al., 2009).

The mammillary bodies are two rounded protrusions that sit behind the tuber cinereum. In the space between mammillary bodies in front and posterior to cerebral peduncles, there is a depressed area of gray matter known as the posterior perforated substance.

The last part of the floor is smooth and slightly concave when seen from inside the ventricle and is located in area between the mammillary bodies anteriorly and aqueduct posteriorly (Morota et al., 2000).

2.1.5.3. The Anterior Wall

The optic chiasm, along with the lamina terminalis, compose the lowest two-thirds of the 3V anterior wall, and this portion is observable from the outside. Upper third is buried by the rostrum of the CC.

Lamina terminalis consists of a thin gray matter strip and also pia matter, which bridges the gap from the upper surface of the optic chiasm inferiorly to the rostrum of the CC superiorly.

On the other hand, the anterior wall of the 3V is composed of the following structures when seen from inside: the optic chiasm inferiorly, then optic recess, then the lamina terminalis, then the anterior commissure, then the interventricular foramen, and lastly body of the fornix superiorly (Wang et al., 2011).

The foramen of Monro is found at a certain point where the dome of the ventricle and the front wall meet on either side. This foramen is a duct that enters between the fornix body superiorly and anteriorly and the thalamus posteriorly and inferiorly into the lateral ventricle and continues inferior to fornix into the 3V as a single channel (Tubbs et al., 2014).

It is a crescent-shaped opening whose size and form are determined by the dimensions of the ventricles. The foramen on either side grows more ovoid as the ventricles expand (Tubbs et al., 2014).

The anterior commissure is a tight band of fibers that runs horizontally anterior to the fornix columns. It has a diameter that ranges from 1.5 mm to 6.0 mm.

The optic recess is a tiny, acute depression between the ventricle's floor and anterior wall. The optic recess is floored with optic chiasm which also form the posterior wall of the recess and separates it from the infundibulum. Lamina terminalis makes up the anterior and superior parts of its wall (Stratchko et al., 2016).

2.1.5.4. The Posterior Wall

The pineal body is the sole anatomical feature visible in the posterior wall when seen from behind, hidden by the splenium of the CC superiorly and by the two thalami laterally. This wall occupies the distance from the suprapineal recess superiorly to cerebral aqueduct inferiorly. The posterior wall comprises, from top to bottom, of the suprapineal recess, then the habenular commissure, then the pineal body and adjacent recess, then the posterior commissure, and lastly the aqueduct of Sylvius when seen frontally within the third ventricle (Stratchko et al., 2016).

The suprapineal recess is located between the upper surface of pineal gland

inferiorly and the lower layer of tela choroidea superiorly. Pineal gland propagates posteriorly towards the quadrigeminal cistern. The pineal gland stalk has two laminae,one upper and one lower. The habenular commissure passes midline through the upper lamina, while the posterior commissure runs in the lower lamina. Between both laminae, the pineal recess extends backward within the pineal body (Feletti et al., 2021).

The posterior commissure serves as the triangle's base, while the central gray matter of the midbrain serves as its two arms, giving the opening of the Sylvius aqueduct its triangular shape (Feletti et al., 2021).

2.1.5.5. The Lateral Wall

The lateral walls of 3V are buried by the two halves of cerebrum and are not noticeable on the brain's surface. The hypothalamus forms its lower part, and the thalamus forms its upper part. The lateral walls feature a shape similar to that of a bird with an open mouth. The round shape of medial aspect of thalamus forms the head; the open mouth protrudes forward and downward and is formed by hypothalamic recesses: the optic recess represents superior beak, while the infundibular recess represents inferior beak (Rhoton, 2007). Hypothalamic sulcus, which is a depression or groove that ranges from Monro foramen anteriorly to Sylvius aqueduct posteriorly, exists between the hypothalamus and thalamic surfaces. The upper boundary of thalamic surfaces is characterized by thin, elevated lines known as striae medullaris thalami (Rhoton, 2007). Habenulae are tiny prominences on thalamic dorsomedial surfaces, situated anterior to the pineal gland.

The habenular commissure connects the habenulae and passes the midline in the upper lamina of the pineal gland.

Massa intermedia, or interthalamic adhesion, extends into the upper part of the lateral wall of 3V and frequently links the opposing two faces of the thalami. It is found in around 75% of indivisuals and is positioned 2.5 to 6.0mm caudal to the interventricular foramen (Patra et al., 2022). The fornix columns develop noticeable elevated areas in the lateral walls of 3V, slightly inferior to the interventricular foramen, but they fade beneath the surface inferiorly (Stratchko et al., 2016).

2.2. The Corpus Callosum

2.2.1. Brief History

Galen wrote about the CC in the 2nd century, and he did it based on his surgical and anatomical dissection experience as a physician. As the majority of his views

based on the anatomy of animals, however, his description missed specificity and was unclear. It served as the only definition of CC till 16th century, when Vesalius enhanced details to offer a more accurate anatomical picture of this structure (Broadfield, 2001). In 1741, a physician called Giovanni Lancisi hypothesized that CC may be the "locus of the soul," as evidenced by the observation that traumatic injuries to the pineal gland may not necessarily result in fatality, whereas harm to the CC may. (Broadfield, 2001).

Ivan Pavlov found in the 1920s that the dogs that were stimulated to secrete saliva in response to stimuli delivered at one of the body's sides also salivated when delivered with the same stimulus at the opposite side (Fearing et al., 1929). As a result, researchers decided to cut the CC in dogs and condition them using the same methods as mentioned above. The importance of the CC in the interhemispheric flow of information was demonstrated by the observation that the dogs showed no signs of bilateral information sharing after their CCs were separated (Broadfield, 2001).

Upon this discovery, other experiments involving the separation of CC in animals were performed to investigate the resulting motor and memory deficiencies.

This has prompted increased investigations of both typical and aberrant development, with an emphasis on the effects of the latter on CC function.

2.2.2. Anatomy Review

The CC is the most prominent commissural portion in the brain, composed of 200 million of highly myelinated fibers that link both cerebral halves (Tanaka-Arakawa et al., 2015). It is about 10 centimeters in length and curves forward and backward along the brain midline. CC develops quickly through the infancy period because of an increase in quantity of axons, axon thickness, and also myelin. Although CC is totally developed at age four, the growth still continues at a considerably slow rate into the third decade of life (Tanaka-Arakawa et al., 2015).

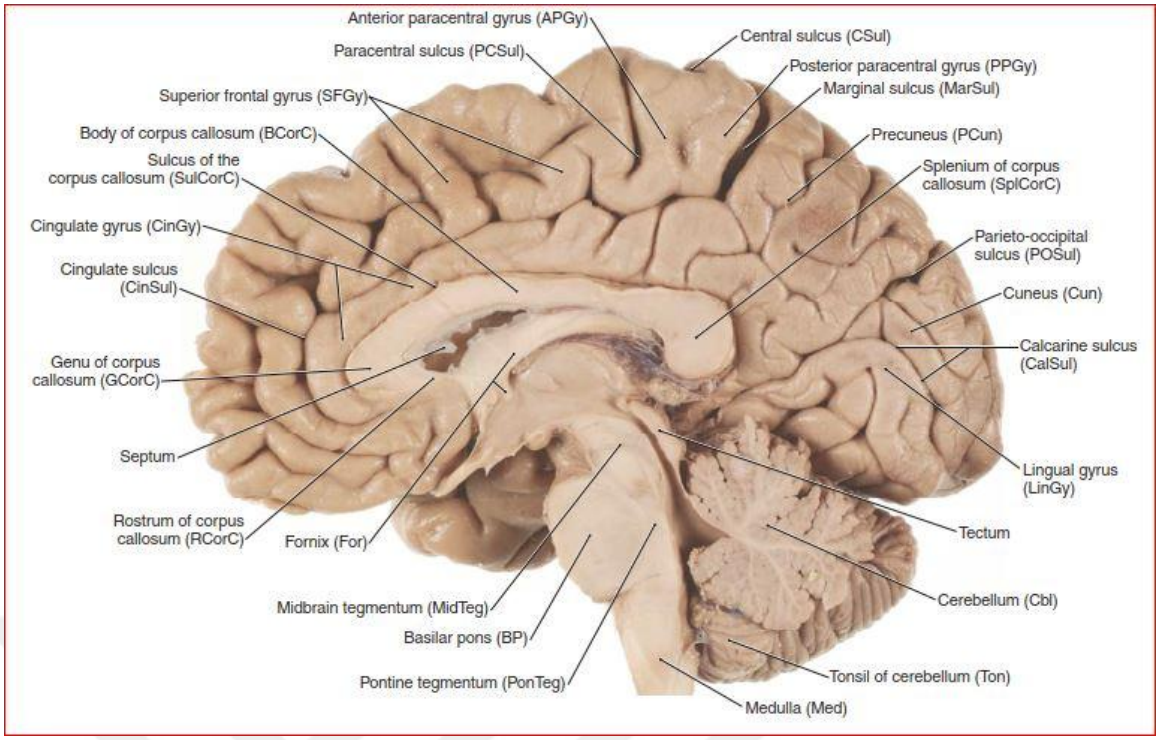

Figure 2. 5. The corpus callosum in midsagittal plane with adjacent structures (Haines, 2015)

The implementation of lateralized sensory information and the integration of higher-level cognitive with social processes rely on the development of accurate interconnections between the cortical and subcortical parts of the brain (Fenlon & Richards, 2015). This is accomplished via midline bridging, a process involving the interaction of newly generated callosal neurons with axon-guidance signals that direct the growth of the callosal axons toward, through, and apart from the midline (Fenlon & Richards, 2015). This causes the CC's topographical arrangement, which in turn permits fibers to link the contralateral areas where the cell bodies are found (Paul, 2011). Expansion of the frontal lobes is proven to cause a gradual forward movement of the CC's anterior boundary during normal development (Pashaj et al., 2013).

Histological studies have identified four separate regions of the corpus callosum that function to establish connections between various portions of the cerebral cortex: the most anterior is the rostrum, followed by the genu, then the body, and lastly the splenium posteriorly, isthmus segment is identified as the thin portion that connects the body with the splenium (Sakai et al ., 2017).

Genu represents the most anterior segment nearly four centimeters from the frontal poles. It is a thicker segment with a sudden direction shift of the fibers from the rostrum to the body. In the midsagittal plane, these fibers constitute the anterior

boundary of the septum pellucidum and are frequently named forceps minor. The ventral part of genu segment bends posteroinferiorly ahead of the septum pellucidum, then thins fast and extends to the upper end of the lamina terminalis as the rostrum. Rostrum joins the orbital surfaces of the frontal lobe and projects from the anterior commissure and extends forewards to the genu. (Raybaud, 2010).

The body of the CC bends outward and terminates posteriorly in the enlarged splenium. The anterior cerebral arteries are supported by the body's median portion, which also forms the base for the longitudinal fissure and lies beneath the falx cerebri's lower edge, which may attach from behind. There is also a thin sheet of gray mutter extending over the upper surface of the CC called the induseum griseum. The cingulate gyrus, on each side covers the body of CC and is separated from it by the callosal sulcus (Raybaud, 2010). Fibers from the precentral cortex with fibers from the cingulate gyrus compose the majority of the body fibers. According to Witelson, the body can be further segmented into an anterior midbody and a posterior midbody (Witelson, 1989). The anterior midbody comprises thicker but less numerous fibers and links premotor and supplementary motor regions, whereas the posterior midbody links primary motor regions with massive, heavily myelinated fibers (Paul, 2011).

The inferior face of the CC is concave throughout its principal axis and connects to the septum pellucidum (Musiek, 1986).

The isthmus is an essential portion of the CC, despite being present in a limited percentage of humans. The isthmus includes fibers from precentral and postcentral gyri and also from the primary auditory region (Bloom & Hynd, 2005).

The splenium is the largest segment of the CC and is positioned around six centimeters from the occipital poles, the pineal gland is hidden by the splenium's ventral surface (Musiek, 1986). The splenium's fibers may also be categorized into three groups: superior, posterior, and inferior groups. The superior one includes fibers for the posterior parietal cortex, whereas the posterior one includes fibers for the medial occipital cortex, and the inferior one includes fibers for the medial cortex of temporal lobe (van der Knaap & van der Ham, 2011). As a group, these fibers form forceps major. The tapetum joins temporal lobes, while the forceps major joins the occipital lobes (Edwards et al., 2014). When the expansion of the splenium is abrupt, it is described as having a bulbous appearance, but when it is gradually expands it is described as having a tubular appearance (Suganthy et al., 2003).

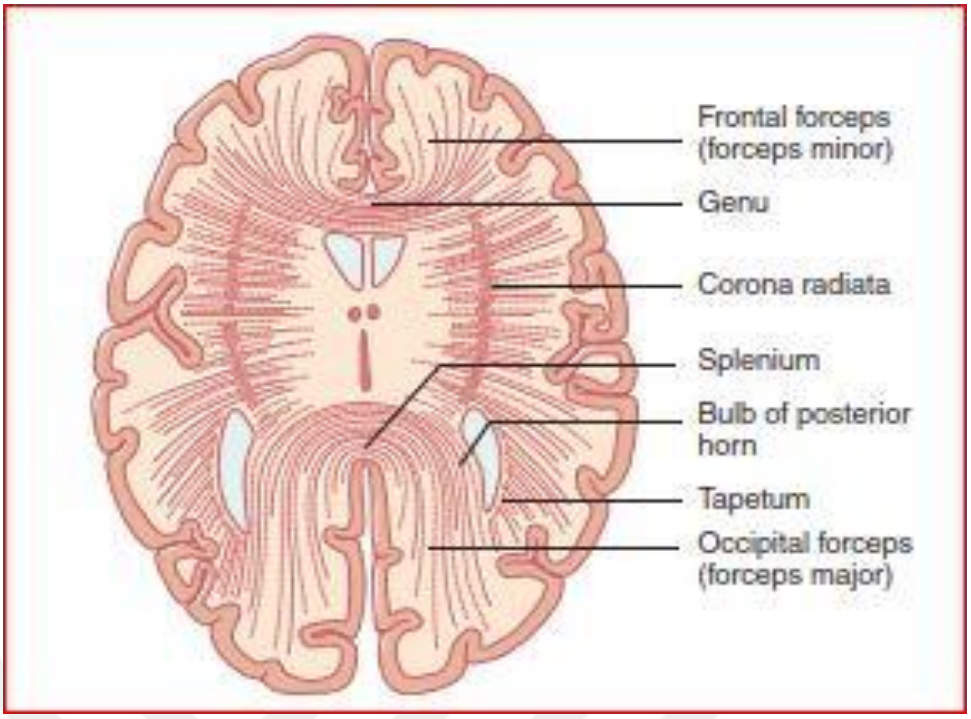

Figure 2. 6. Forceps minor and forceps major (Muti, 2016)

In short, the occipital lobes are linked by the splenial fibers, and the corona radiata is made up of the fibers in the body. The rostrum fibers link the orbital regions together (Musiek, 1986).

The fornix and the lateral ventricles are adjacent to the CC; hence the three structures have close relations. The CC, together with the fornix, serves as an anatomical partition between both lateral ventricles (Musiek, 1986).

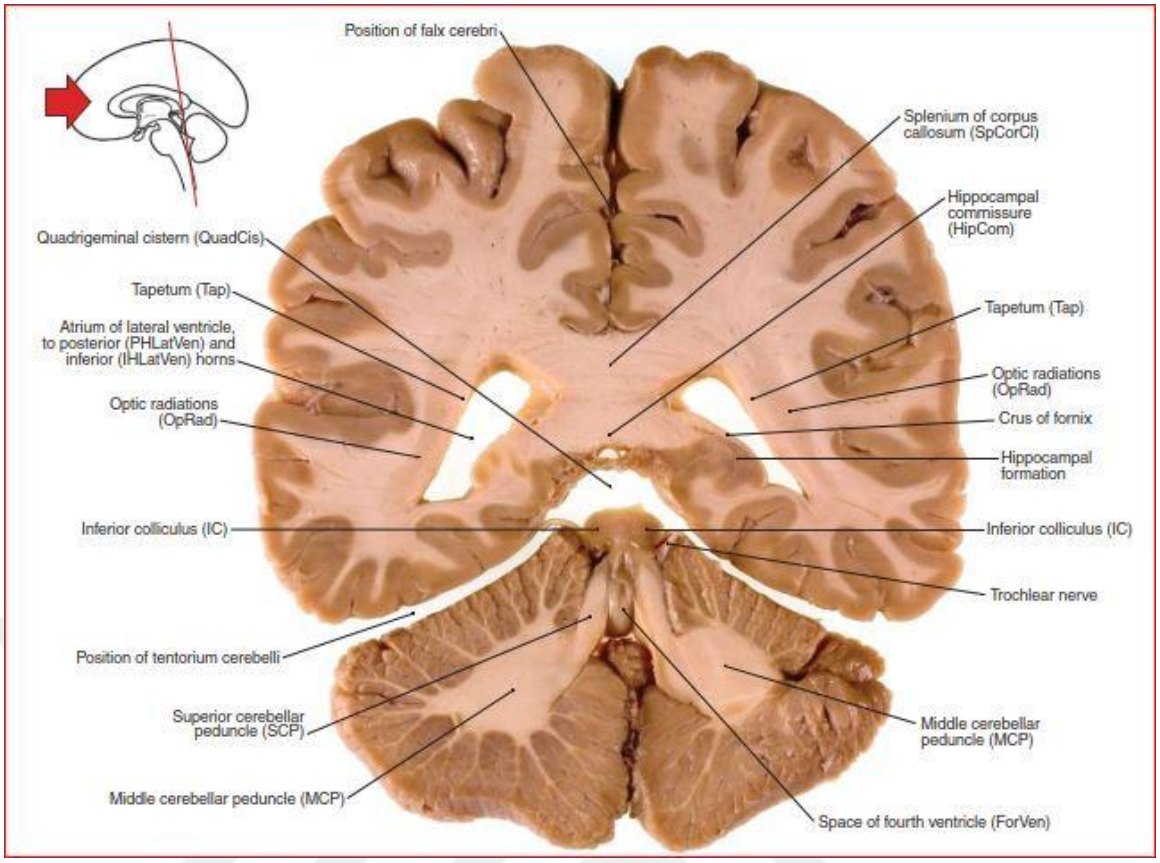

Figure 2. 7. The splenium and tapetum and the relation with lateral ventricle (Haines, 2015)

There are segments of the CC that contribute to the boundaries of the lateral ventricle. The rostrum forms the inferior boundary of the anterior horn, whereas the genu and body of the CC form the anterior and superior borders, respectively, and the body of the CC forms the superior boundary of the central part of the ventricle (Kwon et al., 2014). Age-related expansion of the ventricles has been reported, and since the CC is located so adjacent to the lateral ventricle, it follows that the CC may be susceptible to tension from the expansion of the ventricles (Kwon et al., 2014).

Corpus callosum agenesis and hypoplasia are examples of variations. Rarely occurring, agenesis of the CC causes either the whole or part disappearance of the corpus callosum.

2.2.3. Variation in Corpus Callosum Anatomy

The CC's morphological structure can be used as a diagnostic tool since it changes in response to various disorders. Therefore, a foundation for the diagnosis and monitoring of a disease may be laid with an understanding of CC morphology changes in relation to sex and age. Age- and gender-related morphological differences have been the subject of a significant amount of

investigation and research (Gupta et al., 2008). Obtaining measurements from MR imaging, CT scans, and also autopsies has allowed for the detection of the shape and volume of the CC to be determined. Many recent studies on CC morphology have used MR imaging, which allows for the study of a brain while it is still alive and functional (Mooshagian, 2008). Studies of sexual differences have been shown to be inconsistent. The link between CC and brain size is not constant and might vary across sexes. It is commonly accepted that males have relatively larger bodies and even brains than females, so it is necessary to take brain size into consideration when comparing gender (Sullivan et al., 2001).

2.2.4. Embryology of Corpus Callosum

The corpus callosum is comprised of around 200 million axons (Edwards et al., 2014). The connections that form the corpus callosum are the result of nerve fibers crossing the midline during the 12th or 13th gestational week. Vaginal ultrasound can detect all four CC segments by 18 weeks of gestation (Maccabi et al., 1993). Whether or not the CC grows in the craniocaudal axis is a matter of considerable disagreement; some evidence supports the theory that it does, while others have found the opposite growth trend (Fitsiori et al., 2011). Corpus callosum developed with the neocortex, making its presence among primates a curious universality.

2.2.5. Arterial Supply and Venous Drainage

Branches from the internal carotid artery supply blood to most of the corpus callosum by means of pericallosal artery, which is a branch of the anterior cerebral artery. With the exception of the splenium which receives blood supply from the basilar trunk branches. Splenium receives arterial blood via the posterior cerebral artery through terminal and choroidal branches. Callosal and callosal cingular veins drain venous blood into internal cerebral veins (Fitsiori et al., 2011).

2.2.6. Functions of the Corpus Callosum

The CC's primary role is to facilitate communication between the brain's two hemispheres, namely between the analogous cortical and subcortical regions. There are two primary schools of thought about how the CC affects brain activity: the theory of inhibition, which holds that one hemisphere can suppress the activity of the other, and the theory of excitement, which holds that the opposite is true (Bloom & Hynd, 2005).

The CC allows the right cerebral hemisphere to receive information from and send information to the left side of the body, and vice versa. Each hemisphere's

memory is built on the input and output it gets from the other. As a result, the corpus callosum is responsible for relaying information from the brain's experienced hemisphere to its inexperienced counterpart (Innocenti, 1994).

The four regions of the left cerebral cortex involved in speech production are: Wernicke's area, with the angular gyrus, the supramarginal gyrus, and also Broca's area. All of them are linked to their right-hemisphere counterparts through the corpus callosum.

To interpret sensory, motor, and complex cognitive impulses, the CC must combine and convey information from both cerebral hemispheres. Individuals who underwent callosotomy with either partial or whole hemisphere disconnection have been extensively studied to understand more about the function of the CC. These findings suggest that the CC has a topographical arrangement, with its posterior portions responsible for the transmission of visual, auditory signals, as well as somatosensory , and its anterior portions responsible for the functioning of higher cognition (van der Knaap & van der Ham, 2011). Also, the CC has a significant impact on the development of refined motor skills and higher cognitive abilities as white matter in the brain grows. Furthermore, research has demonstrated that CC provides an inhibiting function that generally suppresses disorganized motor performance of the hands (van der Knaap & van der Ham, 2011).

2.2.7. Partitioning of the Corpus Callosum

Several techniques have been described for CC segmentation, and the variety in methods may be relatively responsible for the inconsistency of the results between different studies (Constant & Ruther, 1996).

Witelson method: Witelson's straight line approach, introduced in 1989, is the primary methodology for CC segmentation. Using this method, a straight line that resembles the maximum anteroposterior diameter, is made (Witelson, 1989). Based on that line the CC is subdivided into seven segments, as shown in figure 2. 8. After the rostrum and genu come the rostral body, the anterior and posterior midbodies, the isthmus, and finally the splenium.

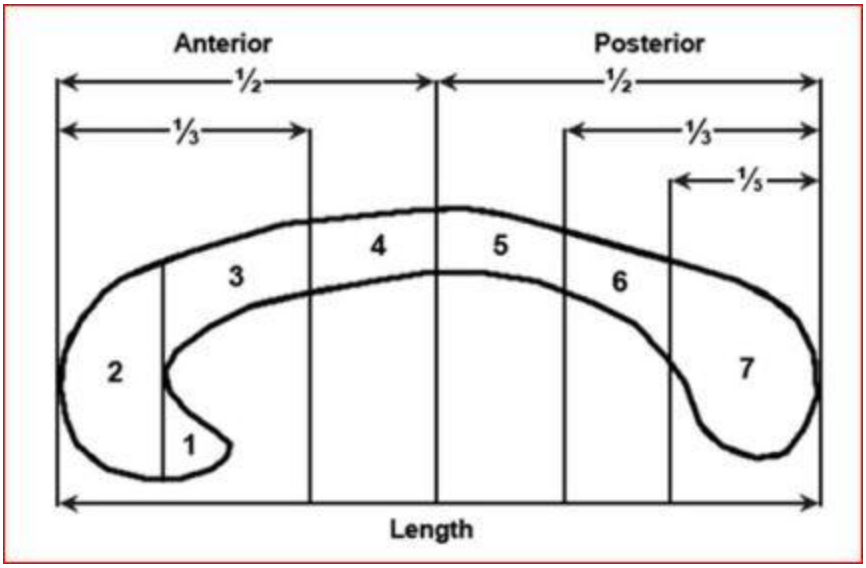

Figure 2. 8. Corpus callosum segmentation in midsagittal plane according to witelson method (Witelson, 1989).

To precisely partition each region, Witelson separated CC into these seven segments based on various fibers orientations; nevertheless, this approach is reliant on the form of the genu and splenium, which might produce ambiguous findings (Tuncer et al., 2005).

Radial partitioning method: As with the previous method, a straight line extends from CC's front to back (Broadfield, 2001). By creating a radial divider that moves every 30 degrees from 0 to 180 degrees, we may split CC into six segments based on the line's midpoint (Ryberg et al., 2006). As a result of this method, the genu and rostrum are taken into account as one entity and treated as the CC's first segment. Though this method successfully subdivides the CC into its constituent parts, its heavy reliance on the CC's shape raises concerns about possible bias (Ryberg et al., 2006).

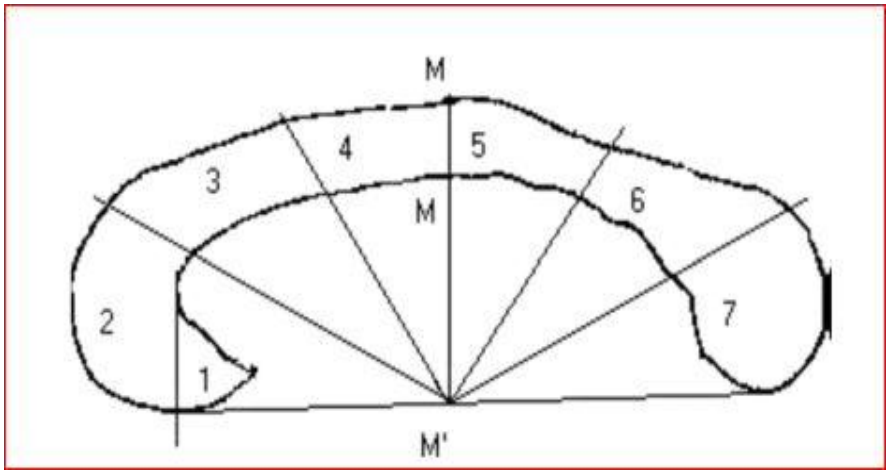

Figure 2. 9. Radial partioning method of corpus callosum (Ryberg et al., 2006).

Curved line method: This method involves calculating the distance starting in the rostrum and ending in the splenium along the arc formed by the midpoints of the upper and lower halves of the CC (Allen et al., 1991). CC may be measured throughout its length and broken down into its five constituent parts. Figure 2.10 illustrates these segments. This approach has the benefit of being independent of the CC's shape, but it might be challenging to draw the line precisely if some areas of the CC are ill-defined (Allen et al., 1991).

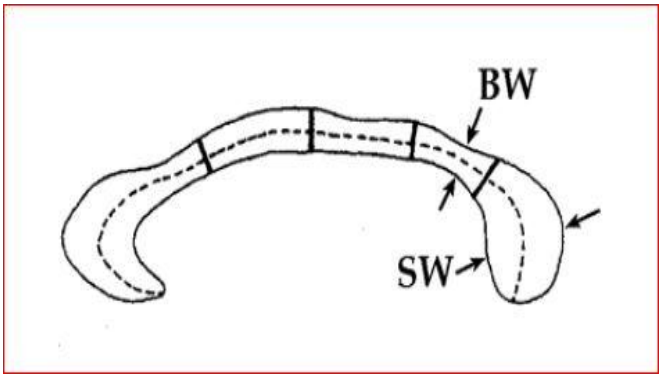

Figure 2. 10. Segmentation of the corpus callosum by curved line method (Allen et al., 1991).

Corpus callosum index (CCI): This idea was proposed by Figueira et al. (2007) in a study that sought to find a measure for the surviellence of MS patients that could be applied easily, recreated by different investigators, and had some sort of evidence of a clinical correlation to assert its anatomical and physiological validity.

Using a basic orthogonal semi-automated approach, we measured the maximum anterior-posterior diameter of the corpus callosum CC and its midline on a standard

best mid-sagittal T1W plane to calculate the CCI (figure 2.11). The anterior, posterior, and middle segment segments of CC were estimated, and their sizes were standardized based on the largest anteroposterior diameter of the whole structure, as in Figure 2.11 (Figueira et al., 2007).

The corpus callosum index CCI was extensively used recently to monitor MS patients. Furthermore, it is easy to apply, and time-saving method, and does not need complex software. For these reasons, this method was chosen to be used in our study.

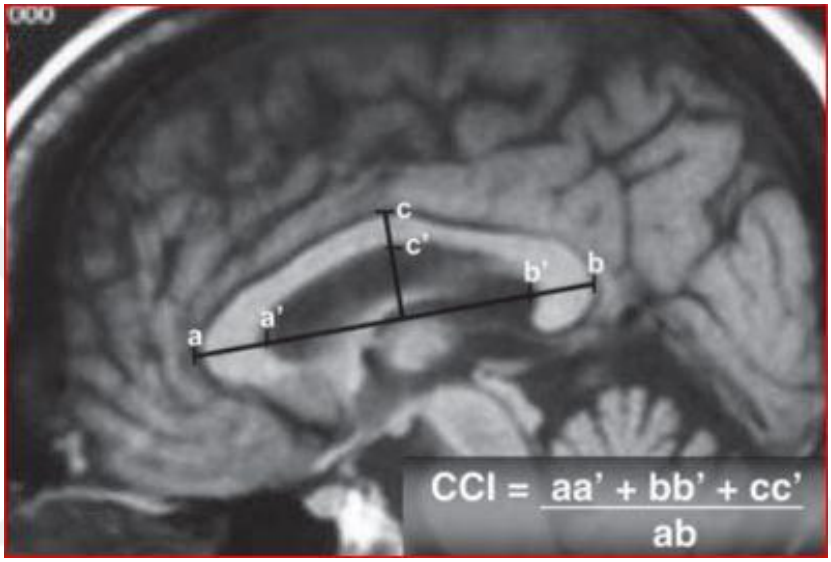

Figure 2. 11. Corpus callosum index (Figueira et al., 2007).

2.3. Multiple Sclerosis (MS)

2.3.1. Introduction to Multiple Sclerosis

MS follows trauma in causing disability in young people (Kobelt et al., 2017). The true origin of the rising prevalence and incidence of MS across industrialized and underdeveloped nations remains uncertain (Browne P. et al., 2014). It is a multifaceted condition that is influenced by a variety of environmental factors as well as a multitude of genes that significantly augment susceptibility to the disease (Alfredsson & Olsson, 2019). Previously, multiple sclerosis was characterized as a T-cell-mediated autoimmune disease. The effectiveness of treatments that target B cells, Conversely, it raises doubts regarding the conventional autoimmune theory of T cells. (Greenfield & Hauser, 2018). The conventional understanding of multiple sclerosis (MS) posits a dichotomous disease process, characterized by two distinct stages. The first stage involves inflammation, which gives rise to relapsing-remitting MS. The second stage involves neurodegeneration, which leads to progression, ultimately culminating in the

primary and secondary progressive forms of MS (Leray et al., 2010). The traditional biphasic model of MS is being significantly contested by the observation that treatments exhibit efficacy across various stages of disease progression (Giovannoni et al ., 2017).

2.3.2. Epidemiology and Etiology

It is commonly asserted that the etiology of MS is undetermined, but this is incorrect. EBV, sunlight (UVB), and smoking, along with an individual's genetic heritage, play an essential role in the pathogenesis of MS (Dobson & Giovannoni, 2019). Immigration research studies frequently indicate that MS is a consequence of environmental exposure (Kurtzke, 2013). Individuals born to migrants in European continent have an increased chance of acquiring disease, whereas adults who leave relatively low-risk countries for Europe face a lower chance of having the disease. It is clear from migration studies that environmental variables are more influential than genetic predisposition, providing significant support for research focusing on preventative strategies that target established environmental dangers (Kurtzke, 2013).

Individuals who are confirmed to be negative for the Epstein-Barr virus (EBV) are shielded from the risk of developing multiple sclerosis (Pakpoor et al., 2013). However, the likelihood of acquiring MS increases by twofold in the presence of a symptomatic EBV infection (Handel et al., 2010). The available evidence on the mechanisms that allow EBV to drive up the risk of MS is varied and diverse. Recently, it has been postulated that EBV-mediated transformation holds significant implications for the pathogenesis of diseases (Tracy et al., 2012).

The prevalence of MS is progressively expanding on a worldwide scale (Browne P et al., 2014). This prevalence exhibits a positive correlation with geographical location. There exists a robust correlation between MS prevalence and the latitudinal gradient, which is attributed to the influence of ultraviolet B (UVB) exposure on the production of vitamin D. The correlation between low levels of vitamin D, reduced intake of vitamin D, decreased outdoor activity, and increased susceptibility to multiple sclerosis (MS) due to genetic polymorphisms that result in low vitamin D levels suggests that vitamin D plays a crucial part in a causal relationship with MS (Sintzel et al., 2018).

The prevalence of multiple sclerosis exhibits a higher incidence rate in the female population; however, historical records indicate that, in the past, things were not always like this. According to case data from the beginning of the 1900s, the

proportion of males and females was nearly equivalent. Subsequently, there has been a consistent rise in the sex ratio, which has now reached approximately 3:1 (Female:Male) in the majority of developed nations (Orton et al., 2006). Based on empirical evidence, smoking has been identified as a factor that increases the likelihood of acquiring multiple sclerosis (MS) by approximately 50%. Moreover, it has been proposed that smoking accounts for up to 40% of the heightened prevalence of multiple sclerosis in women. Prior to the onset of the Second World War, the incidence of smoking among females was relatively infrequent. Subsequent to the war, there was a notable increase in the prevalence of female smokers, which was concomitant with the rising incidence of (MS) among women (Palacios et al., 2011).

An individual's vulnerability to MS is influenced by genetics, with approximately one out of every eight patients having a familial history of the disease (Harirchian et al., 2018). The level of concordance among female monozygotic twins varies across different regions. The concordance rate in the United Kingdom and Canada is approximately 30%, while in southern Europe, it is as low as around 8.5% (Ristori et al., 2006).

2.3.3. Pathology and Immunology

The distinctive pathological feature of MS is the presence of periventricular inflammatory lesions, which subsequently result in demyelinating plaques (Karussis, 2014). The inflammatory infiltrates comprise T-lymphocytes, with the presence of B-cells and plasma cells in relatively decreased quantities (Lassmann, 2013). Early on in the course of the disease, axons tend to remain relatively intact. However, as the disease advances, there is a development of irreversible injury to the axons (Trapp et al., 1998). Although relapsing-remitting MS and progressive MS are clinically distinct, both exhibit pathologically defined inflammatory changes, with relapsing-remitting disease demonstrating a greater degree of inflammation. The phenomenon of remyelination has been observed across all stages of disease, with a higher incidence in cases of progressive disease (Lassmann, 2013). The various subtypes of multiple sclerosis do not exhibit a distinctive histological feature. Rather, there is a variation in the distribution of specific characteristics within different regions. Therefore, although three distinct clinical forms of multiple sclerosis have been delineated, the underlying pathological alterations exhibit a continuous spectrum. This is consistent with the gradual progression of clinical disease observed in patients, wherein they transition from RRMS to SPMS over a span of several years (Dobson & Giovannoni, 2019).

2.3.4. Clinical Picture

The progression of multiple sclerosis entails traversing through various stages, commencing with susceptibility, followed by the asymptomatic, prodromal, and symptoms phases of the condition. There exists a period of vulnerability to multiple sclerosis prior to the onset of preclinical and clinical phases, as indicated by previous research. According to migration research, there exists a temporal gap of 10-20 years between the initial exposure to environmental hazards and the manifestation of related illnesses (Lublin et al., 2014). Depending on pathological investigations, it has been suggested that the preclinical phase of MS may extend over several decades. A Danish study revealed that 25% of individuals who had autopsy pathological confirmation of MS were not diagnosed with the condition during their lifetime (Engell, 1989).

Multiple sclerosis (MS) is commonly considered a potential diagnosis when an individual exhibits symptoms of a clinically isolated syndrome (CIS) (Harirchian et al., 2018). Relapses in individuals with MS typically exhibit a subacute onset spanning from a few hours to several days, followed by a plateauing phase that might remain for a few weeks, and ultimately a gradual recovery. Clinical improvement following relapses in the early stages of MS may seem grossly complete; nevertheless, residual damage is commonly observed after most relapses. The manifestation of symptoms is attributed to the interplay between the dimensions and placement of lesions within the affected area. The visible lesions observed through MRI, also known as macroscopic lesions, represent only a fraction of the total number of lesions present. A significant number of lesions can be detected at the microscopic level, and an even greater number can be found in gray matter of the cortex (Howard et al., 2016). SPMS is known to manifest approximately 10-15 years following the onset of RRMS (Figure 2.12), and is characterized by a gradual transition from sporadic relapses to a more gradual and progressive disease course. The shift between disease forms is not clearly demarcated. Instead, relapses manifest against a backdrop of gradual progression, which precedes the onset of dominant progression. The manifestation of impaired cognition and progressive MRI atrophy in the early stages of MS suggests the presence of neurodegeneration at the onset of clinical symptoms (Mey et al., 2022).

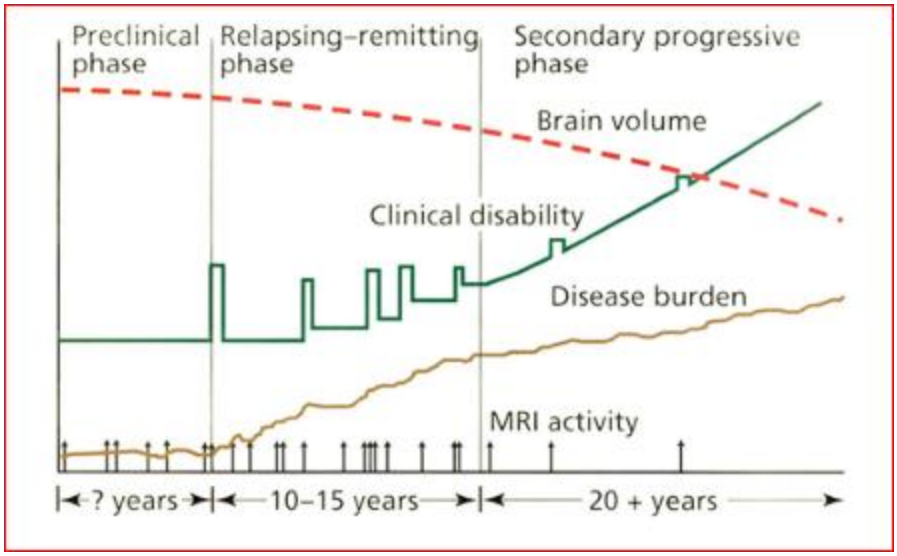

Figure 2. 12. Courses of multiple sclerosis (Mey et al., 2022)

Primary progressive onset (PPMS) occurs in approximately 5% to 15% of instances, and is characterized by a gradual accumulation of progressive disability that primarily affects one dominant neuronal system. The most frequently encountered manifestation involves a gradually worsening spastic paraparesis (Mey et al., 2022).

2.3.5. Diagnosis

The diagnosis of MS is established through a confluence of clinical and radiological characteristics. The McDonald criteria of 2017 serve as the established norm for the diagnosis of various types of the disease (Thompson et al., 2018).

The clinical diagnosis of MS persists as the primary method of identification. It is important to exclude MS mimics through investigations when deemed necessary. It is recommended that patients who are suspected to have MS to undergo a lumbar puncture procedure to aid in confirming diagnosis, ruling out MS mimics, and establishing an elementary prognostic perspective (Thompson et al., 2018).

2.3.6. Magnetic Resonance Imaging (MRI)

It is recommended that all patients receive an MRI scan of the brain at a minimum. In instances where the manifestation is related to the spine, it is recommended to conduct a comprehensive scan that includes the spinal cord. Medical imaging serves a twofold function, as it can serve to corroborate the diagnosis by exhibiting dissemination in both the time and space domains while also ruling out conditions that mimic MS when analyzed by a neuroradiologist with expertise (Hemond & Bakshi, 2018). Specific MRI criteria have been established to facilitate

the early diagnosis of MS in individuals who have experienced only one clinical episode (Polman et al., 2011). A comprehensive understanding of the McDonald criteria necessitates the comprehension of two fundamental concepts. The first aspect to consider is the dissemination in space or DIS, which is characterized on MRI by the detection of at least one lesion in T2 in two of the following four locations: periventricular, juxtacortical, infratentorial, and spinal cord. The second criterion is the dissemination in time or (DIT), which can be identified through MRI as the emergence of a new T2-weighted lesion or Gd-enhancing lesion on a subsequent scan at any given time or the simultaneous appearance of Gadolinium-enhancing and non-enhancing MRI lesions on the initial imaging exam (Kearney et al., 2018). Cooperation between both the neurologist and the radiologist is imperative for accurate diagnosis and optimal management of patients. The clinical information provided to the radiologist is of utmost importance as it plays a crucial role in determining the purpose of the scan, whether it is for diagnostic purposes, monitoring treatment efficacy, or surveillance of adverse reactions. The determination of the scanning protocol to be implemented and the administration of gadolinium are two factors to be considered (Kearney et al., 2018). In cases where a scan is conducted for diagnostic purposes, the administration of gadolinium is deemed necessary to ascertain the presence of DIT. This is particularly relevant for patients with CIS, as it aids in determining whether the diagnosis should be maintained as CIS or upgraded to RRMS (Wattjes et al., 2015). In the context of requesting monitoring scans, it is advisable to provide both the disease subtype and the time interval since the last scan to the radiologist. This enables the radiologist to accurately evaluate the development of any new radiological activity within the appropriate context (Wattjes et al., 2015). In certain cases, patients who do not exhibit any demyelination-related symptoms may display a distribution of lesions in MRI that is consistent with MS. This situation is referred to as Radiologically Isolated Syndrome or (RIS) (Moore, 2009). The utilization of MRI in determining prognosis and evaluating treatment efficacy is extensive. Historically, the quantification of lesions, in conjunction with active lesions that are enhanced by gadolinium, has been employed to approximate the level of disease activity. Nevertheless, the association with long-term outcomes is not entirely accurate (Thompson et al., 2018). Recent advancements in MRI technology, such as diffusion tensor imaging, and functional MRI, have enabled the identification of diseases that exhibit extensive abnormalities beyond the development of focal lesions.

Despite their potential, these techniques have not yet been integrated into routine clinical care (Giorgio and De Stefano, 2016).

2.3.7. Treatment of Multiple Sclerosis

2.3.7.1. Acute Relapses

The primary therapeutic approach for acute relapses is the administration of corticosteroids. The administration of intravenous methylprednisolone is commonly employed, although oral methylprednisolone has demonstrated comparable effectiveness.

Additional alternatives comprise the administration of adrenocorticotropic hormone (ACTH) or the implementation of plasma exchange. Medical intervention is deemed necessary solely in cases where relapse symptoms exert a substantial influence on the individual's quality of life (Berkovich, 2013).

2.3.7.2. Disease-modifying Therapies (DMTs)

The escalation in the quantity and effectiveness of DMTs has sparked a surge of interest in the timely intervention of MS to avoid enduring disability. The therapeutic interventions utilized have been classified as either immuno-suppressant, which includes ocrelizumab, or immunomodulatory, exemplified by teriflunomide. These interventions necessitate continuous treatment in order to sustain the inhibition of inflammation and the progression of the disease. The list of DMTs that are accessible for managing MS continues to increase (Travers and Tsang, 2022).

The selection of the agent is determined by a confluence of patient-related variables such as age, and comorbidities, disease-related factors including the quantity and placement of lesions, and patient preferences regarding the balance between medication side effects and efficacy. Monotherapy with a single DMT has been the standard approach, as there is no empirical evidence to support the efficacy of combination therapy. The utilization of stem cell transplant exhibits significant potential for the effective management of diseases that are unresponsive to conventional treatment methods. (Travers and Tsang, 2022).

2.3.8. The Third Ventricle in Multiple Sclerosis

Third ventricle is a centrally located space that separates the two opposing thalami. 3V expansion may arise due to the degeneration of neighboring anatomical structures, particularly the thalamic regions. Earlier research investigations have proven a correlation between thalamic volume and width of the third ventricle, which has been observed to be enlarged in individuals diagnosed with multiple sclerosis MS

(Cifelli et al., 2002). Disabling effects of multiple sclerosis over time are largely attributed to neurodegenerative processes, as evidenced by previous studies (Roosendaal et al., 2011); accordingly, the thalamus exhibits early signs of atrophy in the brain (Eshaghi et al., 2018).

Patients with MS can be monitored for brain atrophy through various methods. Nevertheless, these methodologies have yet to be incorporated into clinical protocols.

Due to its ease of calculation, the 3V width metric has the potential to be extensively employed in routine clinical practice as an indicator of neurodegenerative processes that manifest as diencephalic atrophy (Guenter et al., 2022).

Cognitive dysfunction manifests in a significant proportion of individuals diagnosed with multiple sclerosis, ranging from 40% to 70%. The underlying pathological mechanisms responsible for cognitive deficits are complicated (Chiaravalloti and DeLuca, 2008). Several studies have demonstrated an association between cognitive decline and various MRI findings in individuals who have multiple sclerosis (MS) (Preziosa et al., 2016).

The research found that there was a correlation between the width of 3V and cognitive impairments such as reduced speed of information processing as well as deficiencies in verbal and visual memory (Guenter et al., 2022). Furthermore, it has been reported that the 3V width exhibited superior prognostic capabilities for verbal memory impairments compared to volumes of the brain, white and gray matter (Benedict et al., 2004).

Some studies reported a correlation of mild to moderate strength between the width of 3V and the Expanded Disability Status Scale (EDSS). The physical disabilities exhibited by individuals with MS have been found to have a correlation with various MRI metrics, including T1 lesion volume and gray matter volume (Roosendaal et al., 2011). Nonetheless, the association between thalamic volume and disability was comparatively less robust than that with cognitive performance (Houtchens et al., 2007).

It has been observed that fatigue can impact a significant proportion of MS patients. This symptom is believed to be linked to thalamus pathology, and research has indicated that the degree of fatigue experienced by MS patients is correlated with the extent of thalamus atrophy (Bernitsas et al., 2017). Prior studies have also indicated that the degeneration of tissue, specifically thalamic degeneration, is more prominent in MS males than females, while that MS males have wider third ventricles (Voskuhl

et al., 2020).

2.3.9. Corpus Callosum in Multiple Sclerosis

Numerous studies have been conducted to estimate CC in the context of MS and is often significantly impacted by ongoing disease.

Its functional importance in facilitating inter-hemispheric communication suggests that it may be a contributing factor in the complicated pathological mechanisms that give rise to cognitive impairments in MS, it can be compromised by focal demyelinating lesions, and even by Wallerian degeneration that arises as a result of axonal loss (Granberg et al., 2015).

The CC can be easily identified through conventional MRI techniques. Its boundaries can be clearly delineated in mid-sagittal images, making it one of the few tracts with well-defined two-dimensional boundaries. Given the anatomical and functional characteristics, it is a justifiable inference that morphometrics of the corpus callosum could serve as a potential indicator for the integrity of associative fibers and reflect pathological processes involved in the onset and progression of multiple sclerosis (Pérez-Martín et al., 2020).

The approaches to CC segmentation have been suggested for evaluating the CC through manual means as linear measurements of the (CCI) and corpus callosum area (CCA) or through volumetric software techniques as the corpus callosum volume (CCV) (Granberg et al., 2015).

Despite the fact that both the CCI and corpus callosum volume CCV exhibited comparable correlation patterns with volumes of brain and MS lesions, the CCV tended to demonstrate superior correlations. It could be argued that the CCV would serve as a more significant biomarker in MS compared to the CCI. Nevertheless, it is crucial to consider that acquiring volumetric data is considerably more challenging than obtaining their linear equivalents (Gonçalves et al., 2018).

The CCI method is considered to be the most readily accessible technique. In addition, a number of studies have exhibited acceptable levels of inter and intra-observer accuracy in relation to this approach (Van Schependom et al., 2016).

Gonçalves et al. revealed a robust association between the CCI and the overall brain volume, primarily due to its relationship with the white matter volume. This finding provides evidence for the reliability of the CCI as an indicator of brain atrophy in individuals with MS (Gonçalves et al., 2018).

2.3.10. Why to Study the Third Ventricle and Corpus Callosum together in Multiple Sclerosis?

The measurement of the widening of the third ventricle in MS patients represents a relevant measurement of the thalamic gray matter because of the close anatomical proximity between the two structures. On the other hand, the white matter bundle of CC is readily distinguishable on conventional MRI, in contrast to many others. As a result, the utilization of manual linear measurements of the CC has the potential to serve as valuable biomarkers for the detection of white matter atrophy (Cappelle et al., 2020).

3. MATERIALS AND METHODS

3.1. Ethical Approval

This study was carried out after gaining permission from the Medical Research Ethics Committee of Ondokuz Mayıs University OMU with the agreement:

B.30.2.ODM.0.20.08/496-569.

It was a retrospective case-control study and used anonymized data after extracting the necessary information. Participants were not engaged beyond the limits that were authorized in this study.

3.2. Source of Data

MRI images of 50 patients were retrieved from the electronic archive of the radiology department in OMU Medical Faculty Hospital.

3.3. Inclusion and Exclusion Criteria

The selected MRIs were performed between 2017 and 2021. The inclusion criteria were: all the patients meet the diagnostic criteria for MS, are already enrolled in a management program, and do not have any exclusion criteria.

Exclusion criteria were: any neurological disease in addition to MS that may affect the gross anatomy of the brain; previous brain surgery, and concurrent or past psychiatric disorders. Age limits were applied to minimize the effect of physiological atrophy of the brain at early and advanced ages. The group of healthy participants was matched with the MS group regarding gender. The subjects in the control group underwent brain MRI for other indications and were proved to be non-remarkable and normal by an experienced radiology specialist.

3.4. Participants

On consulting the statistical department, it was revealed that the least acceptable number for each group is 20 participants after examining some papers that were consistent with related published literature.

Therefore, 25 MS patients whose brain MRIs met the inclusion criteria and who had undergone treatment at our MS referral center were chosen to be studied. The control group consisted of another set of MRI data from a variety of 25 individuals that did not demonstrate any brain pathologies.

3.5. Study Design

This is a monocenter retrospective case-control study.

3.6. MRI Protocol

MRI was used for direct demonstration of the 3V and CC, as MRI has become an established technique in diagnosing and monitoring MS because of its ability to depict the pathologic characteristics of this disease in exquisite details.

A conventional brain MRI scan using a (Philips, Achieva) MRI machine of 1.5 tesla was achieved with the following settings of the machine: TR/TE: 3000/80, the thickness of the slice 5mm, gap 1mm for axial and coronal T1-weighted images.

Regarding T2-weighted sagittal images, the settings were as follows .TR/TE: 600/10, the thickness of slice 5mm, gap 1 mm .

3.7. Images Processing

We used the Radiant program to make the measurements since it is the same tool that is utilized at our radiology department. The sequential MRI data sets were examined using the trial version that was downloaded from radiantviewer.com on a desktop computer. This is dedicated workstation image processing software produced by a Polish company aiming to pursue simplicity in handling medical imaging. This software makes measurements of distances and angles feasible (Figure 3. 1).

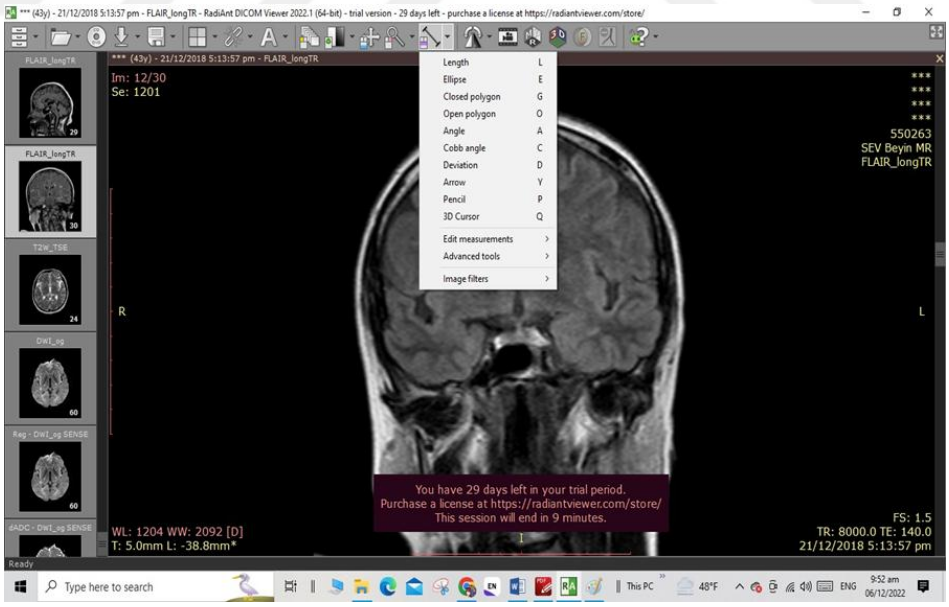

Figure 3. 1. RadiAnt DICOM viewer program

It is simple to use, free for a brief time, and has a user-friendly design. Images and even clips may be exported in a variety of image formats. It includes the following fundamental capabilities for picture alteration and measurement: magnification,

brightness, and contrast adjustment. MRI scan pictures are stored in files in DICOM format.

To minimize measuring mistakes, the observer made the measurements under the guidance of an expert radiologists; as for intra-observer variability, all the measures were evaluated two times with an interval of at least four weeks. The average of the two measurements was utilized to get the final value of each variable. All measurement results in this study were documented in millimeters.

3.8. Third Ventricle Measurements

Five measurements of the 3V were determined in T1-weighted as follows:

3.8.1. Length of the Third Ventricle (L)

It is a line drawn through the long axis of the third ventricle in the axial plane and parallel to the interthalamic fissure where the ventricle is best visualized, as shown in (Figure 3. 2).

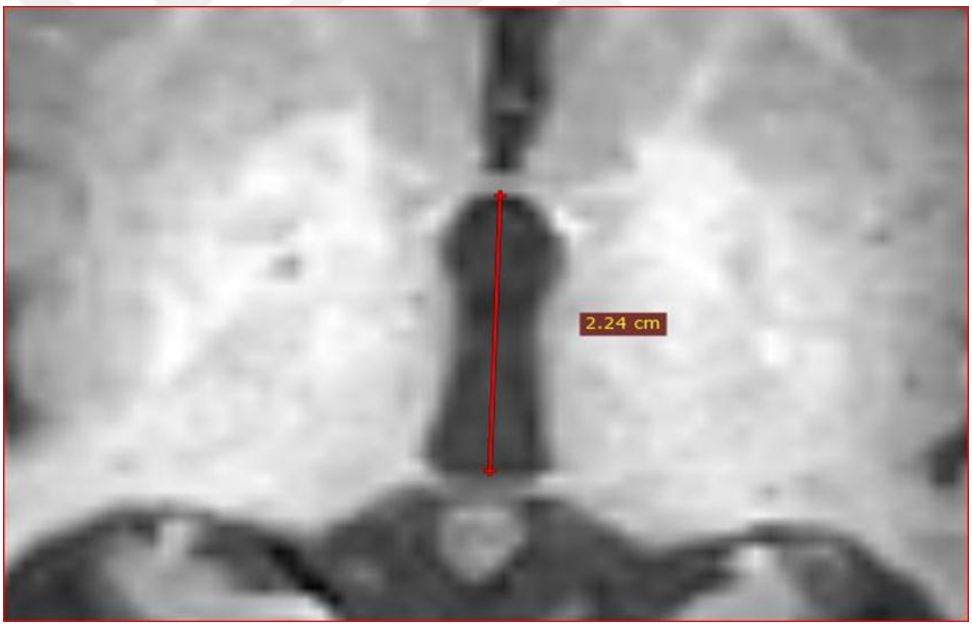

Figure 3. 2. Third ventricle length(L)

3.8.2. Third Ventricle Width (W1)

Measured at the midpoint of the previous line and perpendicular to it (Figure 3. 3).

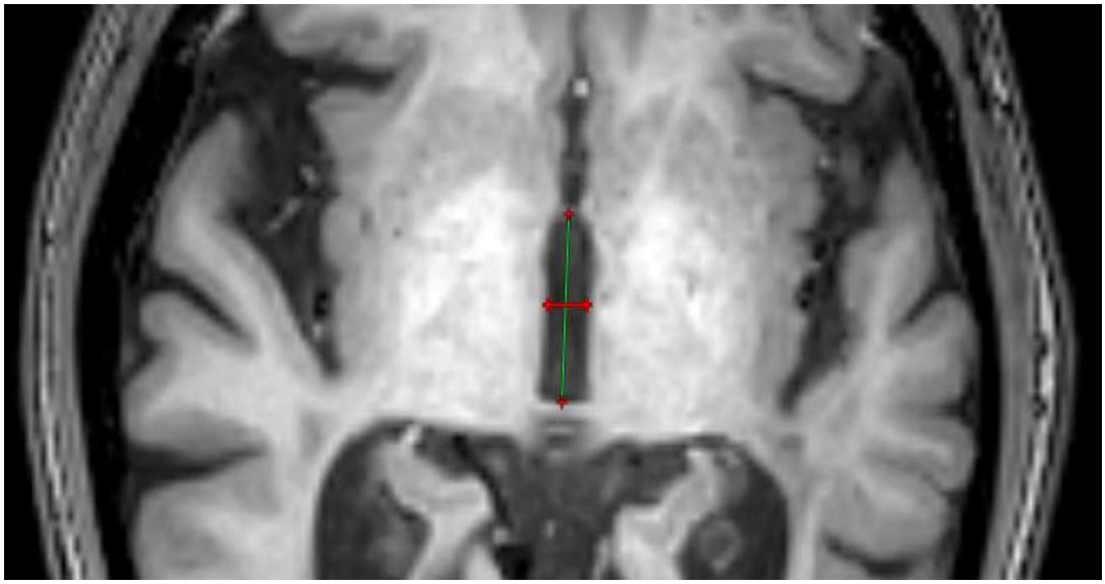

Figure 3. 3. Third ventricle width W1 measured at the midpoint of the anterior-posterior diameter of the ventricle

3.8.3. Third Ventricle Width (W2)

It is defined as the maximum width of the third ventricle that can be measured at the level of the interventricular foramen of Monro in the axial plane (Figure 3.4).

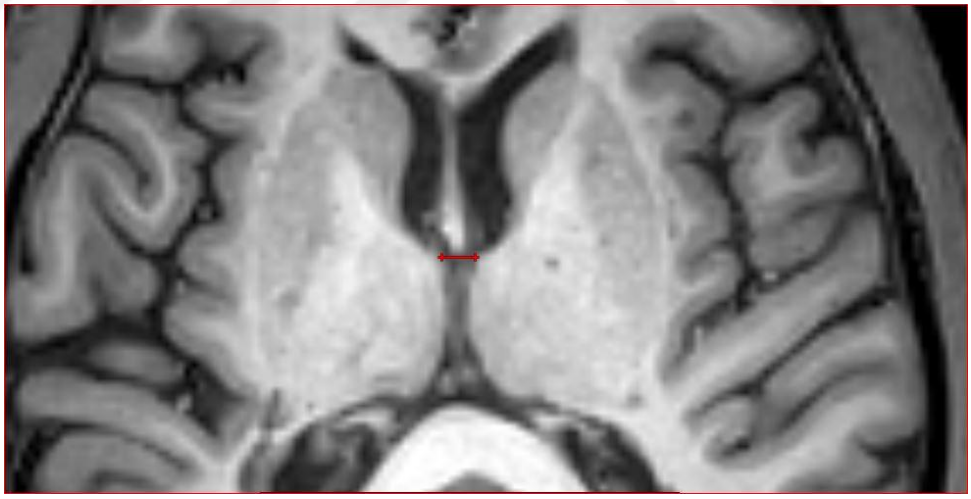

Figure 3. 4. Width of the third ventricle (W2) at the level of the interventricular foramen

3.8.4. Transverse Diameter (TD)

It is the internal transverse diameter of the skull drawn at the same line as (W2) as shown in (Figure 3. 5).

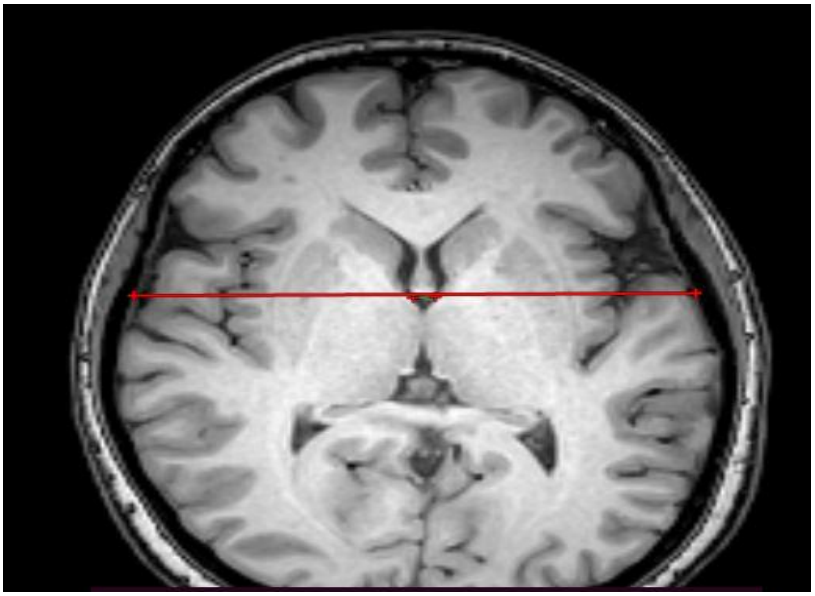

Figure 3. 5. Transverse diameter of the skull (TD)

3.8.5. Third Ventricle Height (H)

It is the maximum height of the 3V that can be measured in the coronal plane, where the foramen of Monro can be visualized (Figure 3. 6).

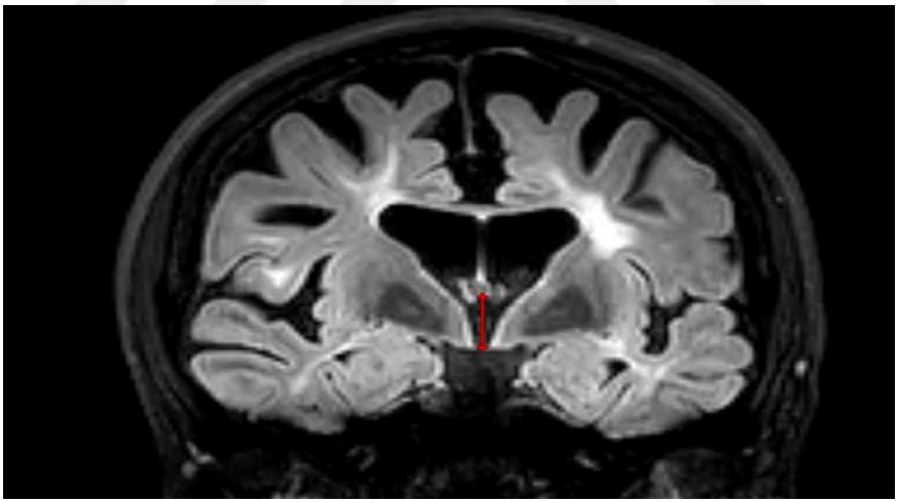

Figure 3. 6. Height of the third ventricle (H)

3.8.6. Third Ventricle Ratio (TVR)

For a more comprehensive evaluation of the third ventricle, we added another parameter to the previous measurements, the third ventricle ratio (TVR). The formula of the ratio is; TVR=W2/TD.

3.9. Corpus Callosum Measurements

The optimal T2-weighted mid-sagittal plane was utilized to visualize the sylvius aqueduct, which serves as a conduit between third and fourth ventricles. On this plane the CC can easily be identified and measured.

The following five variables were considered for CC partioning.

3.9.1. Diameter of the Corous Callosum (AP):

İt is the longest line than can be drawn between anterior and posterior poles of the corpus callosum (Figure 3. 7).

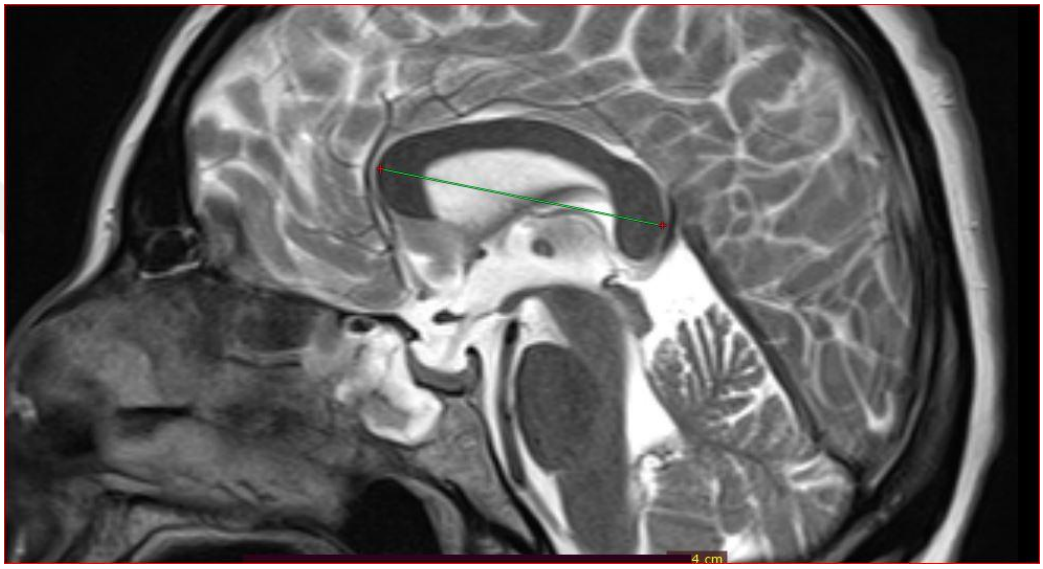

Figure 3. 7. The anteroposterior diameter (AP) corpus callosum

3.9.2. The thickness of genu (G):

It is the measurement of the part of AP diameter that inersects the genu.

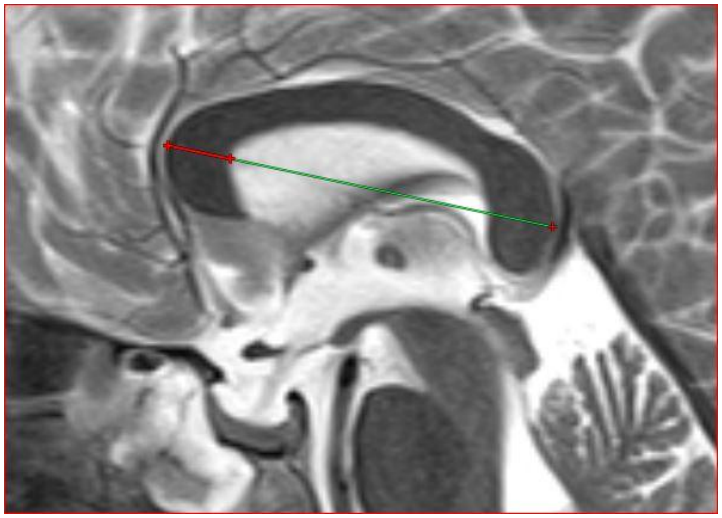

Figure 3. 8. The anterior segment (G) of the corpus callosum

3.9.3. The thickness of splenium (S):

The measurement of the part of AP diameter that intersects the splenium (Figure 3. 9).

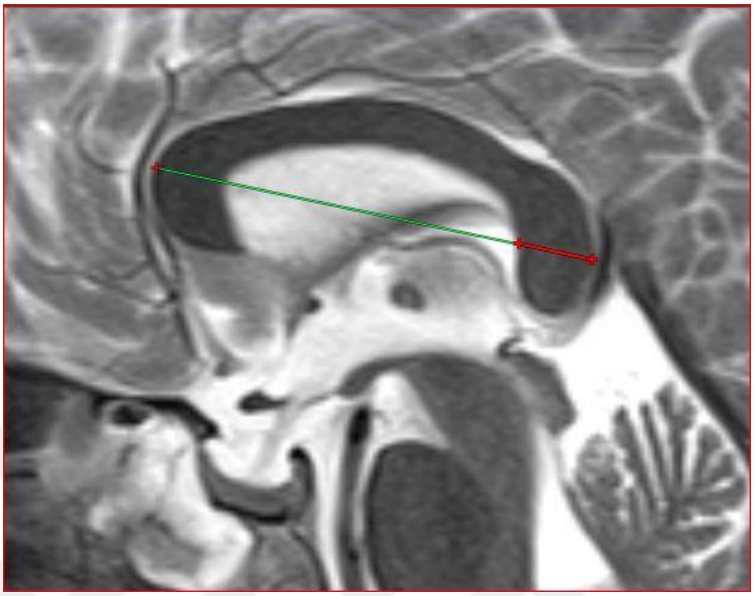

Figure 3. 9. The posterior segment (S) of the corpus callosum

3.9.4. The tkickness of the body (B):

To measure this segment,another line is drawn perpendicular to the AP at its midpoint, so the thickness of body is the measurent of the part of this line that intersects the body (Figure 3. 10).

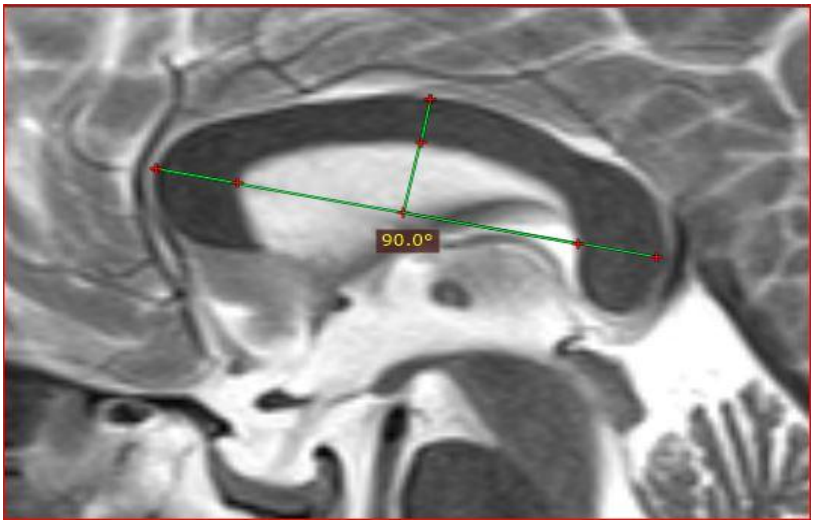

Figure 3. 10. The middle segment (B) of the corpus callosum

3.9.5. Corpos callosum index CCI:

After measuring the semgments of the corpus callosum , then the CCI can easily be calculated through the formula CCI =(G+B+S)/AP.

3.10. Data Analysis

The fundamental clinical and demographic features of the study individuals were examined utilizing SPSS version 25. Various statistical measures were computed, including mean, standard deviation, and also the percentage. Categorical variables, such as gender, were transformed into quantifiable formats for the purpose of statistical analysis using SPSS. Consequently, the male gender was symbolized by value of 1, while the female gender was represented by the value of 2. The Shapiro-Wilk was conducted to check the normality distribution and consequently, to ascertain the appropriate statistical tests to be employed.

Therefore, the study employed a statistical analysis approach to compare the MS group with the control one. Specifically, an independent t-test was utilized for parametric data, while the Mann-Whitney test was employed for non-parametric data. The statistical analyses were deemed significant at a p-value of less than 0.05, with a confidence level of 95%.

Nevertheless, statistical significance merely suggests that there is enough proof to establish that an impact exists. It is a mathematical concept that knows nothing about the given subject or what constitutes a significant influence. Instead, we must apply experience and knowledge to recognize if the influence is strong enough to be important in reality.

4. RESULTS AND DISCUSSION

4.1. Results

4.1.1. Normality Test

According to the Shapiro-Wilk results, all variables had a normality distribution except for gender.

4.1.2. Age and Sex Distribution

The table 4.1 presents a summary of the demographic and fundamental characteristics of both the MS patients and normal controls.

The study comprised of 50 participants whose ages varied between 23 and 48 years. The study involved the categorization of participants into two distinct groups. The first group, referred to as the MS group, consisted of 25 patients, comprising 19 females and 6 males. The average age of the participants in this group was 37 ± 4.08 years. The study's control group comprised 25 participants, of which 20 were females and 5 were males. The control group exhibited a mean age of 33.2 ± 7.51 years, which was comparatively lower than MS group. A significant statistical difference was observed in the age of both groups p=0.04. In relation to gender, the observed results did not exhibit any statistically significant disparity p=0.73.

Table 4. 1. Demographical and fundamental characteristics of participants.

Variables	controls (n= 25)	MS (n= 25)	*P*- value
Age			
Mean	33.2	37	0.04*
(SD)	7.51	4.08	
Gender			
Male	5	6	0.73
Female	20	19	

* Statistically significant

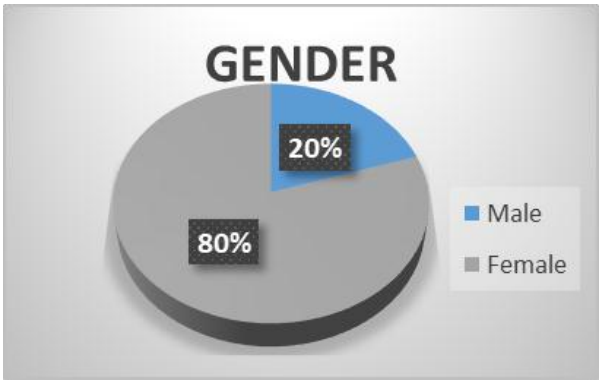

Figure 4. 1. Sex distribution in the control group

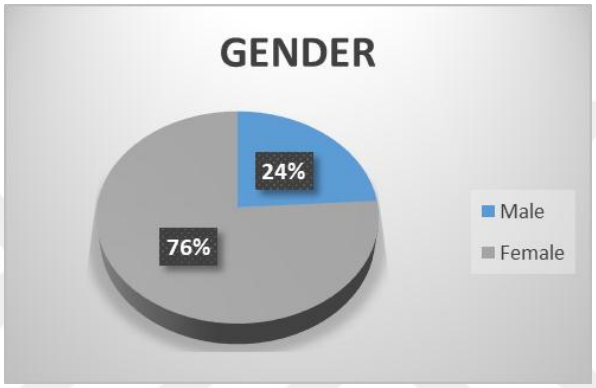

Figure 4. 2. Sex distribution in the MS group

4.1.3. Third Ventricle Variables (L, W1, H)

The clinical characteristics of the three dimensions in the third ventricle are given in (Table 4. 2) below. Three dimensions were used; length (L), width (W1), and height (H).

As explained in the methods section, L is the maximum anteroposterior diameter of the third ventricle that can be measured in the axial plane. W1 is the width of the third ventricle measured at the midpoint of L in the same plane. H is the height of the third vertical measured in the coronal plane where the interventricular foramen can be visualized.

The mean length, width, and height in the MS group were 24.68 ±2.5 mm, 6.08±2.34 mm, and 16.20±1.44 mm respectively. Whereas the mean length, width, and height in the control group were 24.30±1.39 mm, 2.67 ±0.63 mm, and 15.84±092 mm, respectively (Table 4. 2). To evaluate the differences in three dimensions between the two groups, a t- test was performed. The results of the t-test indicated no statistically significant difference between the two groups for L (P = 0.6). Therefore, the hypothesis

that there are no statistically significant differences between the pathological group and the control group for L was accepted. Results indicated that a significant statistical difference existed between both groups with respect to W1 (P=0.001). Therefore, the hypothesis that there are no statistically significant differences between the pathological group and the control group regarding W1 was rejected. As for H (P = 0.21), no statistically significant difference between the two groups was found. Therefore, the hypothesis that there is no statistically significant difference between the two groups was accepted.

Table 4. 2. Measurements of the third ventricle (L, W1, H)

Parameters	Controls (n= 25)	MS (n= 25)	P value
Age			
Min	23	28	
Max	48	44	
Mean	33.2	37	0.04*
(SD)	7.51	4.08	
Width W1			
Min	1.76	2.58	
Max	3.58	12.20	
Mean	2.67	6.08	0.001*
(SD)	0.63	2.34	
Length L			
Min	19.8	18.4	
Max	26.8	30	
Mean	24.30	24.68	0.6
(SD)	1.39	2.50	
Height H			
Min	13.8	12.4	
Max	18.7	19.30	
Mean	15.84	16.20	0.21
(SD)	0.92	1.44	

* Statistically significant

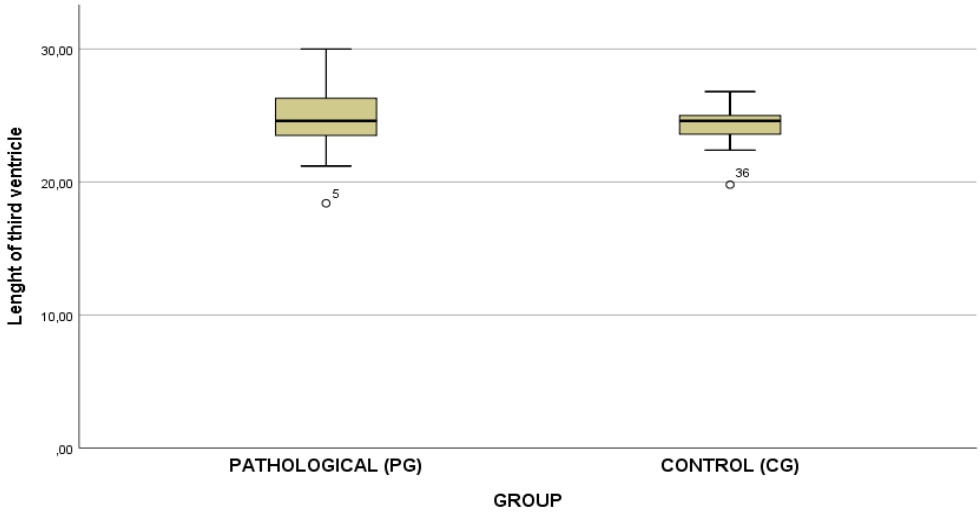

Figure 4. 3. Length of the third ventricle in the MS group and control group

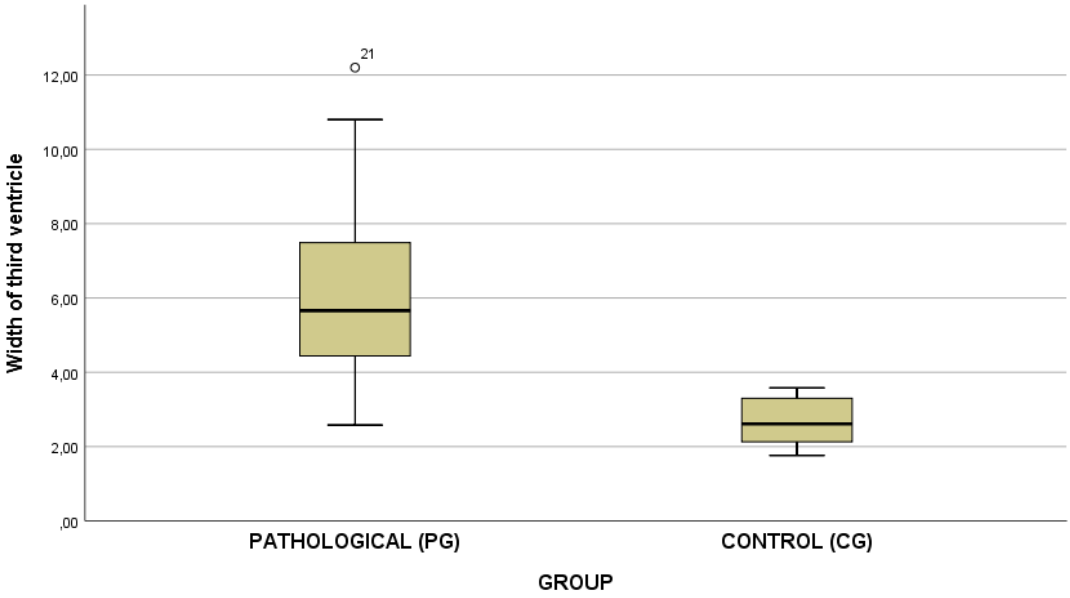

Figure 4. 4. Width W1 of the third ventricle in the MS group and control group.

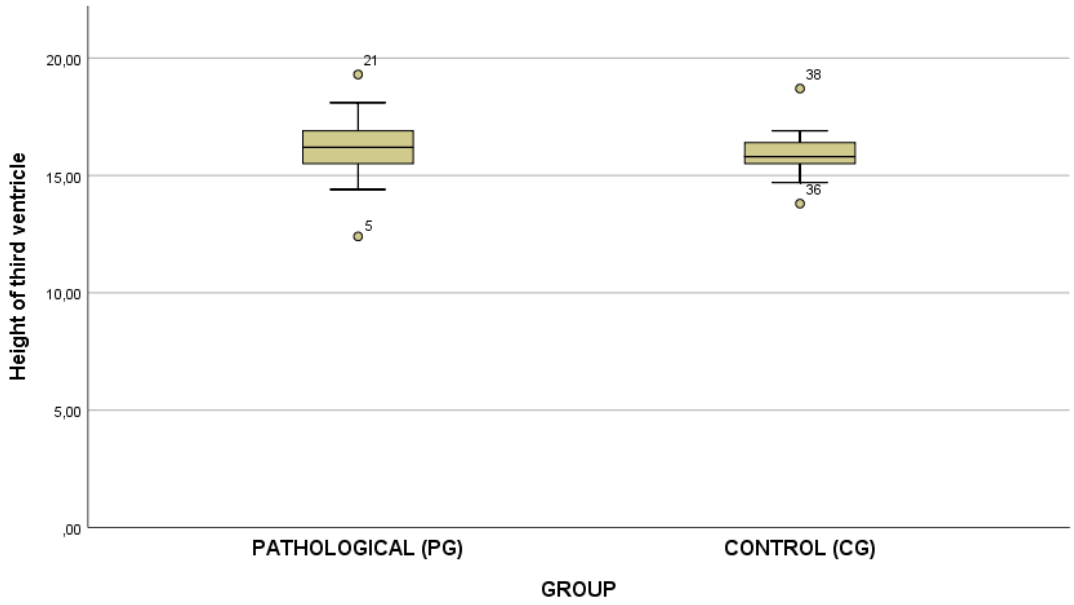

Figure 4. 5. Third ventricle height in the MS group and control group

4.1.4. Third Ventricle Variables (W2, TD, and TVR)

The clinical characteristics of these three dimensions in the third ventricle are given in table 4. 3 below.

The results show that the mean W2, TD, and TVR in the MS group were 6.64±1.85, 125.83±6.93, and 0.05±0.01 respectively. Whereas the mean W2, TD, and TVR in the control group were 3.66±0.64, 125.83±4.79, and 0.03±0.01 respectively. It was concluded from the previous results that the mean W2 and TVR were higher in the patient group than in the control group. Whereas the mean TD in the control group and the patient group was almost the same. To explore the differences in three dimensions between the two groups, a t-test was performed due to normal distribution. The t-test results have revealed a statistically significant distinction between both groups in relation to W2, with a P-value of (0.00). Therefore, the hypothesis that there are no statistically significant differences between the MS group and the control group in W2 was rejected. NO significant difference was noticed regarding TD (P=0.12). Therefore, the hypothesis that there are no statistically significant differences between the two groups in TD was accepted. Finally, the results indicated that there is a statistically significant difference between the MS group and the control group for TVR (P = 0.0). Therefore, the hypothesis that there is no statistically significant difference between the patient group and the control group regarding TVR was

rejected.

Table 4. 3. Measurements of the third ventricle (W2, TD, and TVR) in millimeters.

parameter	Controls (n=25)	MS group (n=25)	*P*-value
Width W2			
Min	2.26	4.11	
Max	5.02	10.8	
Mean	3.66	6.64	0.00*
(SD)	0.64	1.85	
TD			
Min	117.6	108.7	
Max	136.6	137.1	
Mean	125.83	125.83	0.12
(SD)	4.79	6.93	
TVR			
Min	0.02	0.03	
Max	0.04	0.09	
Mean	0.03	0.05	0.02*
(SD)	0.01	0.01	

* Statistically significant

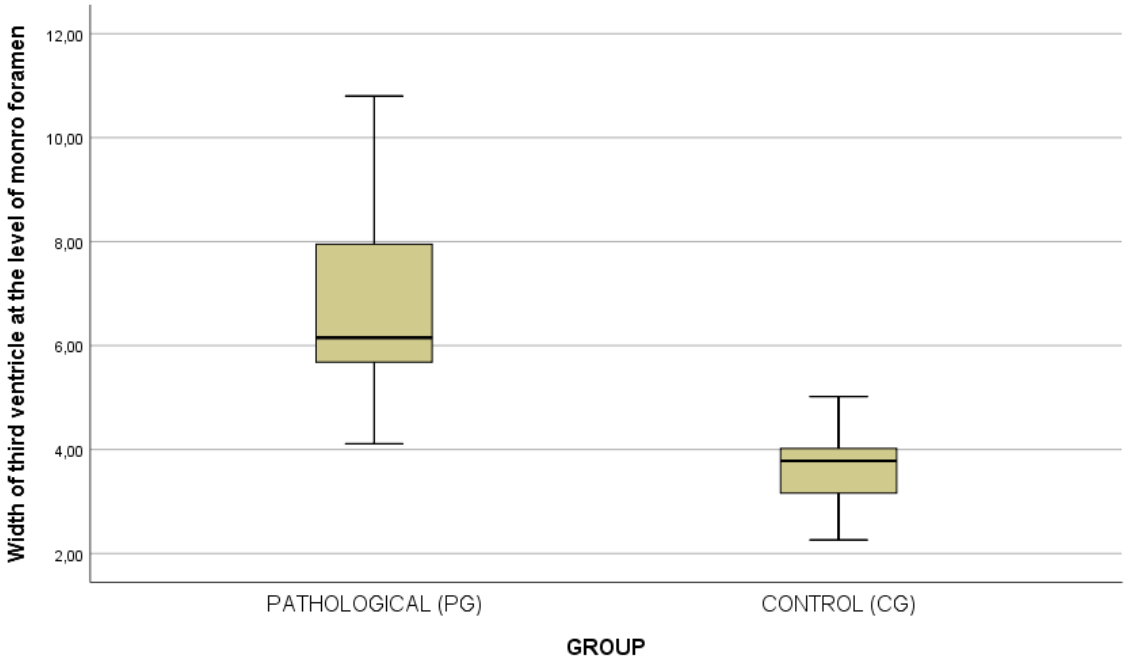

Figure 4. 6. Third ventricle width at the level of the interventricular foramen in MS and control groups

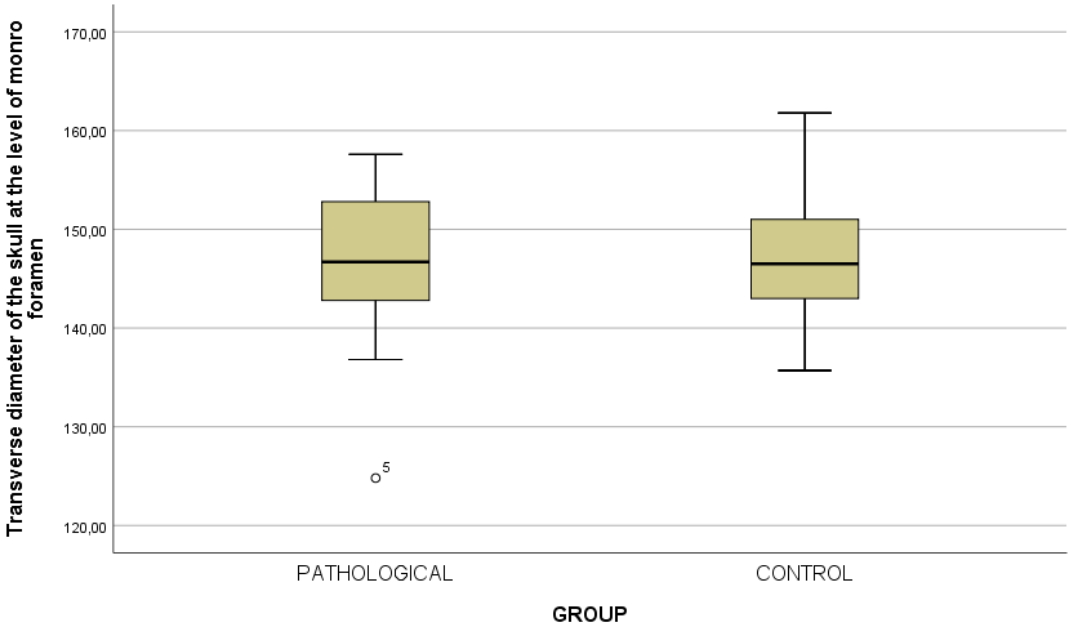

Figure 4. 7. Transverse diameter of the skull at the level of the interventricular foramen in the MS and control groups

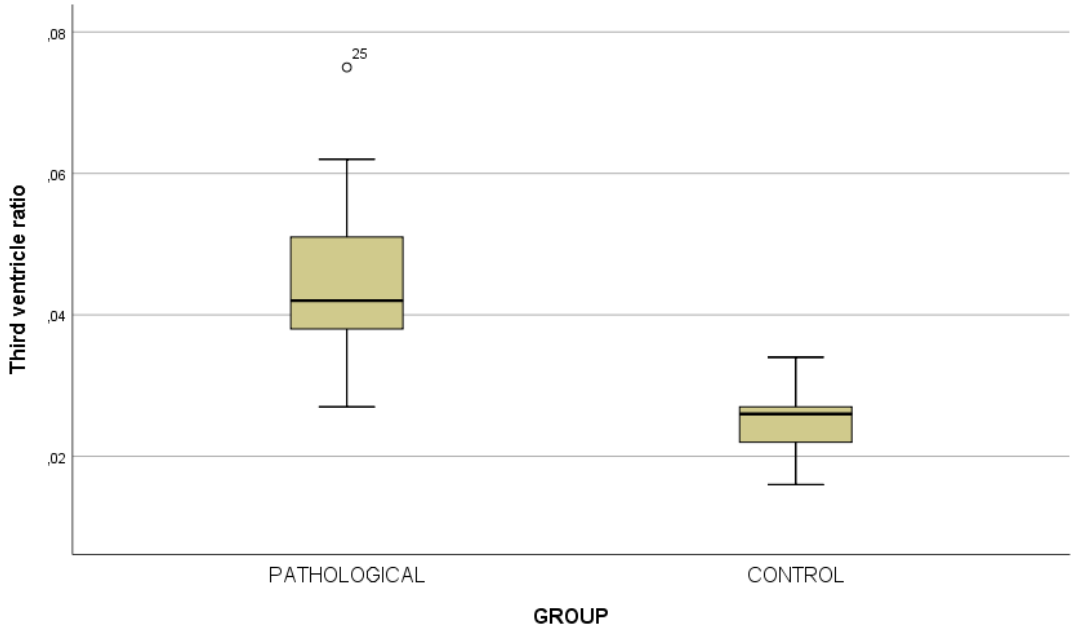

Figure 4. 8. Third ventricle ratio

4.1.5. Measurements of the Third Ventricle in Males and Females

Aiming to compare the measures of 3V of both males and females, we found the results that are summarized in the Table 4.4.

Table 4. 4. Comparison of the third ventricle measurements in males and females in the control group

Control group			
Clinical variables	Male	Female	*p*-value
Number n / (%)	5 / (20%)	20 / (80%)	
L mean-SD	24.76± 0.7	24.18± 1.51	0.42
W1 mean-SD	3.29± 0.37	2.52± 0.59	0.01*
H mean-SD	15.80± 0.66	15.86± 0.98	0.91
W2 mean-SD	3.52± 0.76	3.70± 0.62	0.59
TD mean-SD	128.96± 4.38	125.05± 4.67	0.1

* Statistically significant

Results indicated no significant difference between both with the exception of W1.

Table 4. 5. Comparison of the third ventricle measurements of males and females in MS group

MS group			
clinical variables	Male	Female	*p*-value
Number n / (%)	6 / (24%)	19 / (76%)	
L mean- SD	25.8±2.22	24.32± 2.53	0.21
W1 mean- SD	8.81± 2.45	5.22±1.54	0.00*
H mean- SD	17.1±1.30	15.91± 1.39	0.08
W2 mean- SD	7.8± 1.86	6.27±1.74	0.08
TD mean- SD	130.4± 4.68	124.39± 6.98	0.06

* Statistically significant

Results indicated no significant difference between both with the exception of W1.

4.1.6. Corpus Callosum Variables (G, B, S, AP, and CCI)

The analysis results are summerized in table 4.6. which showed that all the parameters of MS patients were significantly smaller than those of the controls.

Table 4. 6. Measurements of CC in millimeters

Parameters	Controls (n=25)	MS (n=25)	*P*-Value
Age			
mean SD	33.2 ±7.51	37± 4.08	0.04*
Gender M/F	5/20	6/19	0.73
G			
Min	9.380	6.06	
Max	16.70	12.9	
Mean	12.9	9.75	0.000*
SD	1.86	1.85	
B			
Min	5.23	2.17	
Max	9.81	7.51	
Mean	7.54	4.83	0.000*
SD	1.19	1.17	
S			
Min	9.29	4.82	
Max	15.40	14.4	
Mean	13.01	9.96	0.000*
SD	1.53	2.1	
AP			
Min	62.5	55.6	
Max	78.60	75	
Mean	69.72	66.24	0.008*
SD	4.47	4.33	
CCI			
Min	0.40	0.26	
Max	0.58	0.47	
Mean	0.48	0.37	0.000*
SD	0.04	0.06	

* Statistically significant

We also examined the differences between males and females regarding the anatomical parameters of CC, the results were shown in the Table 4.7 and Table 4.8.

Table 4. 7. Comparison between measurements of males and females in the control group

Control group			
Demographic and clinical variables	Male	Female	*p*-value
Number n/(%)	5/(20%)	20/(80%)	
G mean- SD	14.12 ±1.62	12.60±1.8	0.1
B mean- SD	7.46 ±1.43	7.57±1.17	0.11
S mean- SD	12.44±1.34	13.15± 1.57	0.86
AP mean- SD	72.5±4.69	69.02±4.25	0.12
CCI mean- SD	0.47±0.04	0.48±0.04	0.53

Table 4. 8. Comparison between corpus callosum measurements of males and females in MS group

MS group			
Demographic and clinical variables	Male	Female	*p*-value
Number n/(%)	6/(24%)	19/(76)%	
G mean- SD	9.1± 1.88	9.96±1.84	0.32
B mean- SD	4.5±1.1	4.93±1.20	0.43
S mean- SD	9.42±0.91	10.12±2.35	0.49
AP mean- SD	65.37± 2.1	66.52±4.85	0.58
CCI mean- SD	0.35±0.04	0.38±0.06	0.42

Based on these results, there was no significant difference between males and females, neither in control group nor in the MS group.

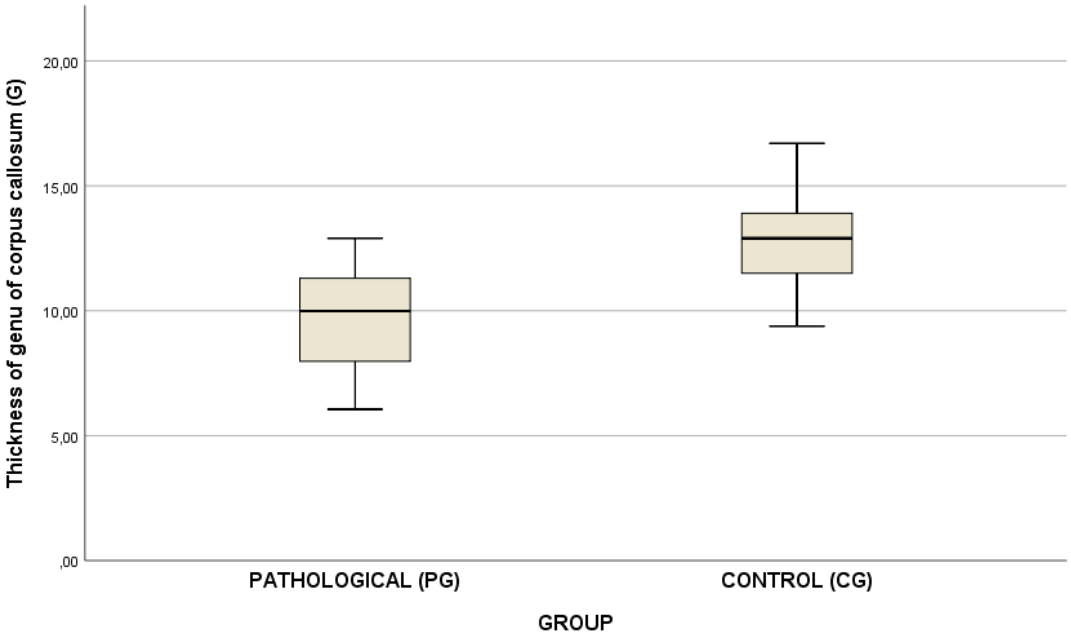

Figure 4. 9. Genu thickness in MS and control group.

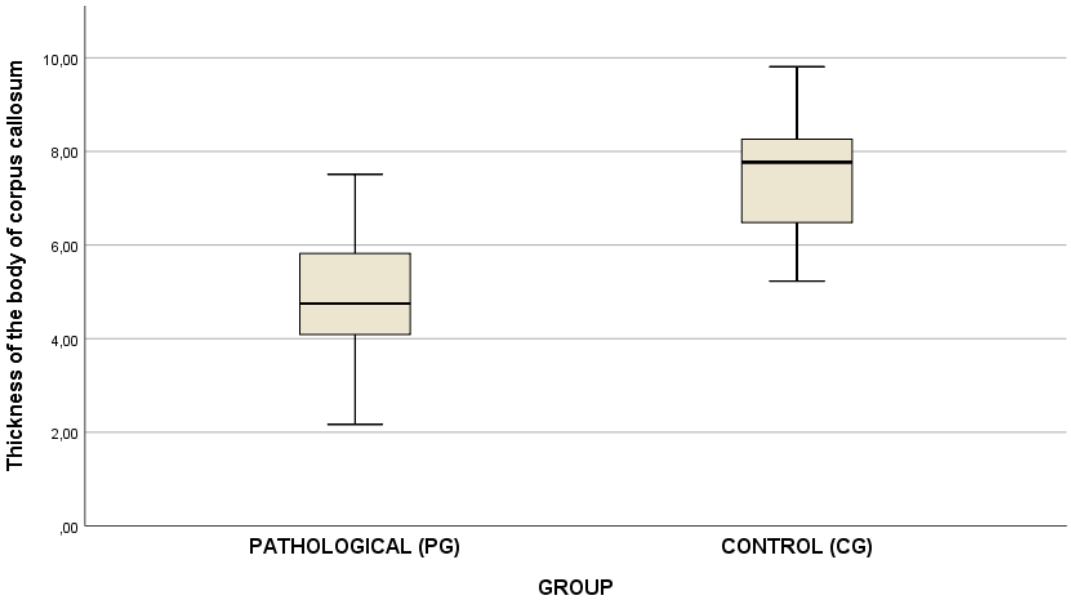

Figure 4. 10. Body thickness in MS and control groups.

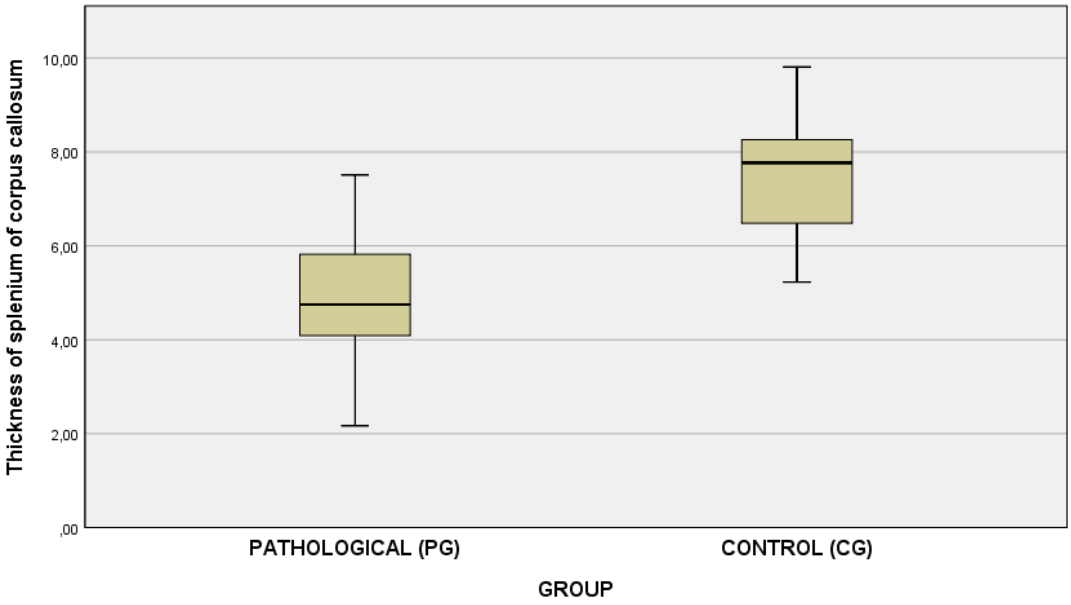

Figure 4. 11. Splenium thickness in the MS and the control group.

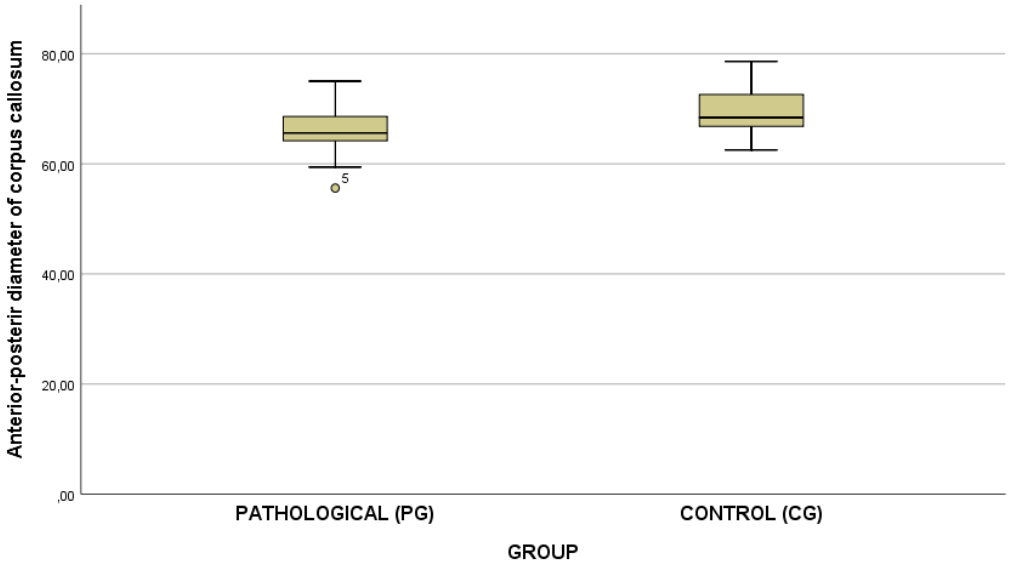

Figure 4. 12. Measurement of AP diameter in the MS and control group.

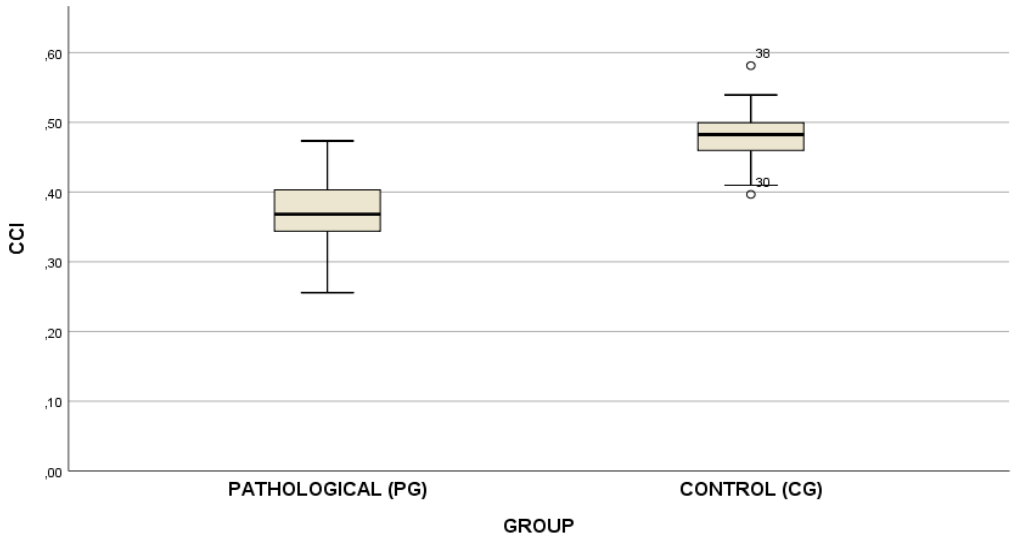

Figure 4. 13. CCI results in the MS and control group

4.2. Discussion

As stated in the introduction, our main aim is to delineate the anatomical changes in the third ventricle and corpus callosum that may occur in multiple sclerosis patients with the help of simple, achievable linear MRI measurements. Conventional MRI has become an established technique for diagnosing and monitoring MS because of its ability to depict the pathologic characteristics of this illness with level of details presented is of exceptional quality and precision.

Despite the existence of multiple techniques for monitoring the atrophy of the brain, manual measures possess the advantage of expeditiously and easily being executed subsequent to the completion of an MRI examination. Many studies have shown that theses measuring techniques exhibits comparable levels of precision to the semiautomatic volume measurement method when assessing the third ventricle and also corpus callosum, debunking earlier research that claimed manual 2D measurements lacked reliability (Lutz et al., 2017).

4.2.1. Third Ventricle Width (W1, W2)

As anticipated, the premier remarkable finding in our study was the widening of 3V in multiple sclerosis patients compared to normal subjects, which is in line with previous studies. Different radiological techniques, including transcranial sonography TCS, CT scan, and MRI, have been used to determine the value of the third ventricle width, but there is no agreement on a minimum and maximum threshold value. It

ranges from 2.25 mm to 9.2 mm, as stated in the literature (Patnaik et al., 2016). As explained in the methods section, we assessed third ventricle width in two different sites and even at two different levels of MRI slices. The mean W1 in MS patients was 6.08± 2.34mm and was measured at the midpoint of the AP diameter of 3V, whereas the mean W2 in MS patients was 6.64 ±1.85 mm and was measured at the level of the interventricular foramen in T1-weighted axial plane.

Schminke et al. assessed the diameter of 3V in 27 MS patients using MRI and TCS. For MRI assessment, they used the same technique that was described for W1, and their results revealed that the mean width was 4.0±1.7 mm (Schminke et al., 2009). Although we used, the same technique and the same sample size and the same mean age (37 years), the measurements in our study were slightly wider. We may explain this by considering that the patients in Schminke's study were in the early stages of the disease, and it may also be because of ethnic disparities. However, we did not take the duration of the disease or the clinical status of patients into account in our study. Schminke et al. also used TCS to measure the transverse diameter of the third ventricle in the same previous MS patients, the mean measurement was 4.4±1.7 mm. Nevertheless, Schminke et al. reported that TCS is not beneficial to monitor disease progression, especially in the early stages of the disease.

Thalamus, which is the main component of the diencephalon, experiences early atrophy in MS (Eshaghi et al., 2018). It is believed that the volume loss of structures adjacent to the third ventricle, specifically thalamus or corpus callosum, causes the 3V to widen (Cifelli et al., 2002). Thus, it reinforces earlier results that third ventricle enlargement may serve as an indirect surrogate for thalamic atrophy in MS. The thalamic nuclei work as a relay station, connecting wide neocortical and subcortical areas and mediating various brain activities. These extensive connections, however, make the thalamus susceptible to retrograde atrophy. This can be brought on by either localized or diffuse brain injury (Houtchens et al., 2007). Consequently, thalamic injury can result in a vast spectrum of neurological symptoms, namely cognitive symptoms (Riccitelli et al., 2011).

4.2.2. Third Ventricle Height (H)

Research has tended to focus on one dimension of 3V, mainly the width of the ventricle, in MS patients. To achieve a comprehensive evaluation of 3V anatomy, we investigated the changes in the height and length parameters in MS patients. The mean height in our study was 15.84 mm in normal participants and resembled the maximum

vertical line drawn in the coronal plane where the interventricular foramen can be visualized. In 2003, Duffner et al. defined the height of the third ventricle as a vertical line passing through the midst of the interthalamic adhesion in the midsagittal plane. He found that the mean height was 18.6 mm in normal controls (Duffner et al., 2003). We argued that we used an easy and practical method as the demonstration of interthalamic adhesion bears some difficulty with a 5 mm MRI slice thickness and even does not exist in all individuals.

In an Ukranian study conducted in 2020, the authors tried to delineate the anatomic parameters of 3V in a normal population by using a brain CT scan and comparing these parameters with the shape of the skull. The definition of the height in this study was the maximum vertical line that can be measured in the mid-sagittal plane. The third ventricle was ordinarily higher among dolichocranial individuals (2.27 ±0.23 cm). The mesocranial group had lower numbers (2.11 ±0.34 cm), while the brachycranial group had the lowest height (2.06± 0.34 cm) (Zhuravlova et al., 2021). All these results were larger than ours, the CT scan is less accurate than MRI in evaluating brain structures, and the age range in the Ukrainian study was larger (21-86 years), with a mean age of 48.6 ±17.57 years, so advanced age may also contributed in third ventricle widening.

4.2.3. Third Ventricle Length (L)

The study findings showed that the mean anterior-posterior diameter of the third ventricle was 24.30±1.39 mm in the control group. Lee et al. used MRI with a 3 mm slice thickness to assess the distance between anterior commissure (AC) and posterior commissure (PC) in the midsagittal plane. Mean AC-PC distance was 26.3±1.79 mm in his control group, with a mean age of 54.74 years (Lee et al., 2008). We may justify this since the mean age in our study (33.2 years) is younger, and the MRI slice is thicker. Also, Lee et al. measured the distance from the center of AC to the center of PC, whereas, we measured the distance from the internal margin of the third ventricle's anterior border to the internal margin of the posterior border.

In a Nepalese study by Dabadi et al. (2020), they evaluated the AC-PC distance in 47 patients with Parkinson's disease using a 3T MRI. They allocated each of AC and PC on the MRI slice in the axial plane, and then the distance was automatically calculated. They reported that the mean AC-PC distance was 24.86±2.08 mm which was very close to our results (Dabadi et al., 2020).

4.2.4. Third Ventricle Ratio (TVR)

The ventricle-brain ratio, which may be estimated using planimetry from brain imaging, is the ratio of total ventricular area to total brain area. It is a frequent measure of ventricular enlargement or cerebral atrophy, and it tends to increase with age. In general, a larger ventricle-brain ratio indicates a worse prognosis for recovering from a brain injury.

It is claimed that the best way to study third ventricle enlargement is to use the third ventricle ratio (TVR), which is established by dividing the third ventricle's width at the level of the interventricular foramen by the skull's internal diameter along the same line (Singh et al., 2018). We found that the mean value of TVR is 0.03±0.01 and 0.05±0.01 in normals and MS patients respectively, with a significant difference (p=0.02). Virsham Singh et al. reported that on normal CT scans, the mean TVR was 0.062 ±0.02 which was greater than the value of TVR in our study of 0.03±0.01. This is because the mean width of the ventricle was 6.51±2.25 mm in his study and 3.66±0.64 mm in ours. He also reported that (TVR) can be used as a screening test for hydrocephalus in suspected individuals.

In another study published in 2020, Khanal and colleagues calculated the TVR for 100 participants with normal CT brain scans. The mean TVR was 0.03±0.01 with a mean ventricle width of 0.3±0.09 cm as it was measured at the level of the superior colliculus (Khanal et al., 2020).

To compare our results of third ventricle variables, based on gender, no significant difference was noticed except for W1. In an Ukrainian study (Zhuravlova & Kornieieva, 2021), the observer reported that the length of the ventricle is larger in males than females in a sample of the Ukrainian population; the same results were reported in a Nigerian study (Bello et al., 2013).

Table 4. 9. The length of the third ventricle

Study	Males	Females
Ukrainian study	23.7±0.40mm	20.8±0.32mm
Nigerian study	27.84±1.53mm	25.42±1.43mm
Our study	24.76±0.7mm	24.18± 1.51mm

The same previous Ukrainian study revealed that the width of the ventricle is larger in males than in females. That finding was also strengthened by an Indian study

(Patnaik et al., 2015).

Table 4. 10. Third ventricle width

Study	Males	Females
Ukrainian study	6.1±0.24 mm	5.0±0.19 mm
Indian study	7.47±2.81mm	6.39±2.6mm
Our study	3.29±0.37mm	2.52±0.59mm

The comparative research poses a challenge in making robust inferences on ethnic disparities in the third ventricle due to varying limitations. The observed variations can be attributed to dissimilarities in research methodology, sample size, and the proportion of male and female participants across the studies.

4.2.5. Corpus Callosum Variables

Several techniques have been described for CC segmentation , and the variety in methods may be relatively responsible for the inconsistency of the results between different studies (Constant & Ruther, 1996).

The present research employed CCI as a means of segmenting corpus callosum. Figueira's findings indicated that the CCI was user-friendly, did not necessitate the use of intricate software, and exhibited sensitivity to the callosal loss of volume. Consequently, it exhibited potential for deployment in the extended surveillance of MS patients.

The present study involved the measurement of various parameters including mean genu thickness (G) which was 9.75 ± 1.85 mm , mean body thickness (B) which was 4.83 ±1.17 mm, mean of splenium thickness (S) that was 9.96 ± 2.1 mm, and the mean of (AP) diameter that was 66.24 ± 4.33 mm. These were obtained results for the MS group . Respectively, the CCI value was found to be 0.37 ± 0.06.

Perez-Alvarez et al. conducted a study in Spain wherein they examined 109 patients diagnosed with multiple sclerosis. The researchers determined corpus callosum index (CCI) for the patients, which was found to be 0.377, consistent with the findings of our own study (Perez-Alvarez et al., 2018).

Regrettably, akin to the majority of clinical trials, the Spanish investigation did not specify the measurements of the segments of corpus callosum , so there was no no possibility for comparative analysis with our study.

Conversely, control group exhibited a mean thickness of G 12.9±1.86 mm , mean thickness of B 7.54 ± 1.19 mm, mean thickness of S 13.01 ± 1.53 mm, mean AP diameter 69.72± 4.47mm , and also the CCI was found to be 0.48 ± 0.04.

In their study, Allouh et al assessed corpus callosum subregions of 100 young adult Arabs from the Middle East, with a mean age of 32 years. The measurements were obtained and reported as in the follwing order with their respective uncertainties: genu thickness was10.9 ± 1.4, body thickness was 6.2 ± 0.8, splenium thickness was 16.6 ± 2.3, and the mean of antrior-posterior AP was 68.4 ± 4.0. Upon comparison, it is evident that all factors, with the exception of the splenium thickness, exhibit decreased values in comparison to our own population. Notably, the Arap population displayed a wider splenium thickness (Allouh., 2020). Allouh's findings were consistent with those of a previous Turkish study conducted by Karakaş et al. (2011). It is noteworthy to mention that Allouh et al. employed a distinct methodology for corpus callosum partitioning (Karakaş et al., 2011).

Regarding CC sex dimorphism, we could not find a difference between males and females in both groups. Sex dimorphism of the CC has been extensively researched with a variety of results in different studies, The available evidence suggests that men tend to possess greater absolute volumes of gray and white matter and that the total size of the CC is also larger in men. This observation aligns with the expectation that men would have bigger brain sizes overall (Shiino et al., 2017). The comparative research presents challenges in drawing robust conclusions regarding racial disparities in corpus callosum due to varying limitations. The observed variations can be attributed to dissimilarities in research method, size of the population , and gender distribution across the studies.

4.2.6. Limitations

In order to enhance the level of assurance, it is imperative to underscore specific constraints and limitations that we encountered throughout the course of the study. Recognizing these challenges, the study's results could be properly regarded as valid and in accordance with the study's basic objectives.

Given that our research is retrospective, we were unable to establish a correlation with clinical status of the individuals, as well as the advancement of MS disease.

One limitation of our study is the relatively small sample size. This is noteworthy given that anatomical variations in 3V and CC have been observed even among individuals without pathology.

Given that multiple sclerosis typically impacts individuals in their early adulthood, the age bracket examined in this study was somewhat limited, ranging from 23 to 48 years. Therefore, in order to ensure the generalizability of the findings, it would be advisable to investigate a broader range of age groups.

An additional constraint pertains to the thickness of MRI slices. In the majority of cases, a 5 mm thickness was employed, with an inadequate resolution.

Despite any potential limitations, the obtained outcomes remain significant in terms of addressing the research inquiry.

5. CONCLUSION AND RECOMMENDATIONS

It is asserted that the present study possesses unique characteristics, as we used simple and easy-to-take MRI linear measurements to evaluate anatomic alterations in 3V and CC in patients suffering MS. They are time-saving measures and do not need special complex software. Also, we implied some measures of the third ventricle that are not usually covered in similar studies. Some of these measurements are already implicated in everyday clinical practice, like width of the 3V and CCI, other measures are not usually covered in studies that deal with MS patients. We investigated the third ventricle in three dimensions: width, length, and height. Width of the ventricle was significantly wider in pathological group, although it was estimated in two different levels. With regard to length and height we did not find a difference from the normal population.

As for the corpus callosum, we found that all the evaluated segments; the genu, the body, and the splenium were atrophied in comparison with normal population; the same is true for the anterior-posterior diameter.

The enhanced measurements will yield more accurate information, facilitating the advancement of novel treatment modalities for third ventricle and corpus callosum diseases. Additionally, these measurements will serve as a valuable tool for physicians to detect deviations from typical anatomical parameters, allowing for early diagnosis and prompt initiation of treatment.

It is recommended that a longitudinal study be conducted with an extended period and a greater number of participants to strengthen the findings pertaining to the clinical context, MS disease variants.

REFERENCES

Alfredsson, L., and Olsson, T. (2019). Lifestyle and environmental factors in multiple sclerosis. *Cold Spring Harbor Perspectives in Medicine*, *9*(4). https://doi.org/10.1101/cshperspect.a028944

Allen, L. S., Richey, M. F., Chai, Y. M., and Gorski, R. A. (1991). Sex differences in the corpus callosum of the living human being. *Journal of Neuroscience*, *11*(4), 933–942. https://doi.org/10.1523/jneurosci.11-04-00933.1991

Amiri, H., de Sitter, A., Bendfeldt, K., Battaglini, M., Gandini Wheeler-Kingshott, C. A. M., Calabrese, M., Geurts, J. J. G., Rocca, M. A., Sastre-Garriga, J., Enzinger, C., de Stefano, N., Filippi, M., Rovira, Á., Barkhof, F., and Vrenken, H. (2018). Urgent challenges in quantification and interpretation of brain grey matter atrophy in individual MS patients using MRI. *NeuroImage: Clinical*, *19*(2017), 466–475. https://doi.org/10.1016/j.nicl.2018.04.023

Andravizou, A., Dardiotis, E., Artemiadis, A., Sokratous, M., Siokas, V., Tsouris, Z., Aloizou, A.-M., Nikolaidis, I., Bakirtzis, C., Tsivgoulis, G., Deretzi, G., Grigoriadis, N., Bogdanos, D. P., and Hadjigeorgiou, G. M. (2019). Brain atrophy in multiple sclerosis: mechanisms, clinical relevance and treatment options. *Autoimmunity Highlights*, *10*(1). https://doi.org/10.1186/s13317-019-0117-5

Aydin, S., Yilmazlar, S., Aker, S., and Korfali, E. (2009). Anatomy of the floor of the third ventricle in relation to endoscopic ventriculostomy. *Clinical Anatomy*, *22*(8), 916–924. https://doi.org/10.1002/ca.20867

Bello, S., Abdulhameed, A., Bello, S., Bello, A., Usman, J., Zagga, A., Tadros, A., Yunusa, G., Saidu, S., and Ahmed, H. (2013). Morphological variation of third ventricle using computerized tomography among different gender and age groups: A 5-year retrospective study in Usmanu Danfodiyo University Teaching Hospital, Sokoto, North - West Nigeria. *Sahel Medical Journal*, *16*(3), 83. https://doi.org/10.4103/1118-8561.121904

Benedict, R. H. B., Weinstock-Guttman, B., Fishman, I., Sharma, J., Tjoa, C. W., and Bakshi, R. (2004). Prediction of Neuropsychological Impairment in Multiple Sclerosis. *Archives of Neurology*, *61*(2), 226. https://doi.org/10.1001/archneur.61.2.226

Berkovich, R. (2013). Treatment of Acute Relapses in Multiple Sclerosis. *Neurotherapeutics*, *10*(1), 97–105. https://doi.org/10.1007/s13311-012-0160-7

Bernitsas, E., Yarraguntla, K., Bao, F., Sood, R., Santiago-Martinez, C., Govindan, R., Khan, O., and Seraji-Bozorgzad, N. (2017). Structural and neuronal integrity measures of fatigue severity in multiple sclerosis. *Brain Sciences*, *7*(8), 1–10. https://doi.org/10.3390/brainsci7080102

Bloom, J. S., and Hynd, G. W. (2005). The role of the corpus callosum in interhemispheric transfer of information: Excitation or inhibition? *Neuropsychology Review*, *15*(2), 59–71. https://doi.org/10.1007/s11065-005-6252-y

Broadfield, D. C. (2001). *Sex differences in the corpus callosum of Macaca fascicularis and Pan troglodytes*. City University of New York.

Browne, P., Chandraratna, D., Angood, C., Tremlett, H., Baker, C., Taylor, B.V., and Thompson, A.J. (2014). Atlas of Multiple Sclerosis 2013: A growing global problem with widespread inequity. *Neurology*, *93*(11), 1022–1024. http://www.msif.org/about-ms/publications-

Bruni, J. E., Del Bigio, M. R., and Clattenburg, R. E. (1985). Ependyma: Normal and pathological. A review of the literature. *Brain Research Reviews*, *9*(1), 1–19. https://doi.org/10.1016/0165-0173(85)90016-5

Cappelle, S., Pareto, D., Tintoré, M., Vidal-Jordana, A., Alyafeai, R., Alberich, M., Sastre-Garriga, J., Auger, C., Montalban, X., and Rovira, À. (2020). A validation study of manual atrophy measures in patients with Multiple Sclerosis. *Neuroradiology*, *62*(8), 955–964. https://doi.org/10.1007/s00234-020-02401-3

Chiaravalloti, N. D., and DeLuca, J. (2008). Cognitive impairment in multiple sclerosis. *The Lancet Neurology*, *7*(12), 1139–1151. https://doi.org/10.1016/S1474-4422(08)70259-X-Cifelli, A., Arridge, M., Jezzard, P., Esiri, M. M., Palace, J., & Matthews, P. M. (2002). Thalamic neurodegeneration in multiple sclerosis. *Annals of Neurology*, *52*(5), 650–653. https://doi.org/10.1002/ana.10326

Constant, D., and Ruther, H. (1996). Sexual dimorphism in the human corpus callosum? A comparison of methodologies. *Brain Research*, *727*(1–2), 99–106. https://doi.org/10.1016/0006-8993(96)00358-7

Dabadi, S., Dhungel, R., Dhungel, P., Gurung, P., Shrestha, R., Acharya, S., Rajbhandhari, P., Shrestha, P., and Pant, B. (2020). Study of anterior commissure-posterior commissure distance among Nepalese cohort. *Asian Journal of Neurosurgery*, *15*(04), 966–969. https://doi.org/10.4103/ajns.ajns_232_20

Dezena, R. A., Juratli, T. A., Aguiar, P. H. P. de, Reis, R. G. D., Oliveira, J. P. de O. J. de, Nyarko, O. Y., Santos, L. N. Q., and Aguiar, P. H. S. de P. de. (2020). Anatomy of the ventricular system: Historical and morphological aspects. *Archives of Pediatric Neurosurgery*, *2*(1), 35–43. https://doi.org/10.29327/apn.v2i1(january-april).23

Dobson, R., and Giovannoni, G. (2019). Multiple sclerosis – a review. *European Journal of Neurology*, *26*(1), 27–40. https://doi.org/10.1111/ene.13819

Duffner, F., Schiffbauer, H., Glemser, D., Skalej, M., and Freudenstein, D. (2003). *Clinical Article Anatomy of the cerebral ventricular system for endoscopic neurosurgery : a magnetic resonance study*. 359–368. https://doi.org/10.1007/s00701-003-0021-6

Edwards, T. J., Sherr, E. H., Barkovich, A. J., and Richards, L. J. (2014). Clinical, genetic and imaging findings identify new causes for corpus callosum development syndromes. *Brain*, *137*(6), 1579–1613. https://doi.org/10.1093/brain/awt358

Engell, T. (1989). A clinical patho- anatomical study of clinically silent multiple sclerosis. *Acta Neurologica Scandinavica*, *79*(5), 428–430. https://doi.org/10.1111/j.1600-0404.1989.tb03811.x

Eshaghi, A., Marinescu, R. V., Young, A. L., Firth, N. C., Prados, F., Jorge Cardoso, M., Tur, C., De Angelis, F., Cawley, N., Brownlee, W. J., De Stefano, N., Laura Stromillo, M., Battaglini, M., Ruggieri, S., Gasperini, C., Filippi, M., Rocca, M. A., Rovira, A., Sastre-Garriga, J., … Ciccarelli, O. (2018). Progression of regional grey matter atrophy in multiple sclerosis. *Brain*, *141*(6), 1665–1677. https://doi.org/10.1093/brain/awy088

Evangelou, N., Konz, D., Esiri, M. M., Smith, S., Palace, J., and Matthews, P. M. (2000). Regional axonal loss in the corpus callosum correlates with cerebral white matter lesion volume and distribution in multiple sclerosis. *Brain*, *123*(9), 1845–1849. https://doi.org/10.1093/brain/123.9.1845

Fearing, F., Pavlov, I. P., and Anrep, G. V. (1929). Conditioned Reflexes. An Investigation of the Physiological Activity of the Cerebral Cortex. In *Journal of the American Institute of Criminal Law and Criminology* (Vol. 20, Issue 1, p. 153). https://doi.org/10.2307/1134737

Feletti, A., Fiorindi, A., Lavecchia, V., Boscolo-Berto, R., Marton, E., Macchi, V., De Caro, R., Longatti, P., Porzionato, A., and Pavesi, G. (2021). A light on the dark side: In vivo endoscopic anatomy of the posterior third ventricle and its variations in hydrocephalus. *Journal of Neurosurgery*, *135*(1), 309–317. https://doi.org/10.3171/2020.4.JNS20493

Fenlon, L. R., and Richards, L. J. (2015). Contralateral targeting of the corpus callosum in normal

and pathological brain function. *Trends in Neurosciences*, *38*(5), 264–272. https://doi.org/10.1016/j.tins.2015.02.007

Fernandes-Silva, J., Silva, S. M., Alves, H., Andrade, J. P., and Arantes, M. (2021). Neurosurgical anatomy of the floor of the third ventricle and related vascular structures. *Surgical and Radiologic Anatomy*, *43*(12), 1915–1925. https://doi.org/10.1007/s00276-021-02785-8

Figueira, F. F. A., Dos Santos, V. S., Figueira, G. M. A., and Da Silva, Â. C. M. (2007). Corpus callosum index: A practical method for long-term follow-up in multiple sclerosis. *Arquivos de Neuro-Psiquiatria*, *65*(4 A), 931–935. https://doi.org/10.1590/s0004-282x2007000600001

Filippi, M., and Rocca, M. A. (2011). MR imaging of multiple sclerosis. *Radiology*, *259*(3), 659–681. https://doi.org/10.1148/radiol.11101362

Fisniku, L. K., Chard, D. T., Jackson, J. S., Anderson, V. M., Altmann, D. R., Miszkiel, K. A., Thompson, A. J., and Miller, D. H. (2008). Gray matter atrophy is related to long-term disability in multiple sclerosis. *Annals of Neurology*, *64*(3), 247–254. https://doi.org/10.1002/ana.21423

Fitsiori, A., Nguyen, D., Karentzos, A., Delavelle, J., and Vargas, M. I. (2011). The corpus callosum: White matter or terra incognita. *British Journal of Radiology*, *84*(997), 5–18. https://doi.org/10.1259/bjr/21946513

Gabrion, J. B., Herbuté, S., Bouillé, C., Maurel, D., Kuchler-Bopp, S., Laabich, A., and Delaunoy, J. P. (1998). Ependymal and choroidal cells in culture: Characterization and functional differentiation. *Microscopy Research and Technique*, *41*(2), 124–157. https://doi.org/10.1002/(SICI)1097-0029(19980415)41:2<124::AID-JEMT3>3.0.CO;2-U

Gazzaniga, M. S. (2000). Cerebral specialization and interhemispheric communication. Does the corpus callosum enable the human condition? *Brain*, *123*(7), 1293–1326. https://doi.org/10.1093/brain/123.7.1293

Ghione, E., Bergsland, N., Dwyer, M. G., Hagemeier, J., Jakimovski, D., Paunkoski, I., Ramasamy, D. P., Carl, E., Hojnacki, D., Kolb, C., Weinstock-Guttman, B., and Zivadinov, R. (2019). Aging and Brain Atrophy in Multiple Sclerosis. *Journal of Neuroimaging*, *29*(4), 527–535. https://doi.org/10.1111/jon.12625

Ghione, E., Bergsland, N., Dwyer, M. G., Hagemeier, J., Jakimovski, D., Paunkoski, I., Ramasamy, D. P., Silva, D., Carl, E., Hojnacki, D., Kolb, C., Weinstock-Guttman, B., and Zivadinov, R. (2018). Brain atrophy is associated with disability progression in patients with MS followed in a clinical routine. *American Journal of Neuroradiology*, *39*(12), 2237–2242. https://doi.org/10.3174/ajnr.A5876

Giorgio, A., and De Stefano, N. (2016). Advanced Structural and Functional Brain MRI in Multiple Sclerosis. *Seminars in Neurology*, *36*(2), 163–176. https://doi.org/10.1055/s-0036-1579737

Giovannoni, G., Cutter, G., Pia-Sormani, M., Belachew, S., Hyde, R., Koendgen, H., Knappertz, V., Tomic, D., Leppert, D., Herndon, R., Wheeler-Kingshott, C. A. M., Ciccarelli, O., Selwood, D., di Cantogno, E. V., Ben-Amor, A. F., Matthews, P., Carassiti, D., Baker, D., and Schmierer, K. (2017). Is multiple sclerosis a length-dependent central axonopathy? The case for therapeutic lag and the asynchronous progressive MS hypotheses. *Multiple Sclerosis and Related Disorders*, *12*, 70–78. https://doi.org/10.1016/j.msard.2017.01.007

Gonçalves, L. I., dos Passos, G. R., Conzatti, L. P., Burger, J. L. P., Tomasi, G. H., Zandoná, M. É., Azambuja, L. S., Gomes, I., Franco, A., Sato, D. K., and Becker, J. (2018). Correlation between the corpus callosum index and brain atrophy, lesion load, and

cognitive dysfunction in multiple sclerosis. *Multiple Sclerosis and Related Disorders*, *20*, 154–158. https://doi.org/10.1016/j.msard.2018.01.015

Granberg, T., Shams, S., Aspelin, P., Kristoffersen-wiberg, M., and Fredrikson, S. (2015). *MRI-Defined Corpus Callosal Atrophy in Multiple Sclerosis : A Comparison of Volumetric Measurements , Corpus Callosum Area*. *Lv*, 1–6. https://doi.org/10.1111/jon.12237

Greenfield, A. L., and Hauser, S. L. (2018). B-cell Therapy for Multiple Sclerosis: Entering an era. *Annals of Neurology*, *83*(1), 13–26. https://doi.org/10.1002/ana.25119

Guenter, W., Betscher, E., and Bonek, R. (2022). Predictive Value of the Third Ventricle Width for Neurological Status in Multiple Sclerosis. *Journal of Clinical Medicine*, *11*(10), 2841. https://doi.org/10.3390/jcm11102841

Gupta, T., Singh, B., Kapoor, K., Gupta, M., and Kochhar, S. (2008). Age and sex related variations in corpus callosal morphology. *Nepal Medical College Journal : NMCJ*, *10*(4), 215–221.

Haines, D. E. , (2015), Neuroanatomy In Clinical Context An Atlas Of Structures, Sectıons And Syndromes, Wolters Kluner Health, P. 28 and 83. ISBN: 978-1-4511-8625-3

Handel, A. E., Williamson, A. J., Disanto, G., Handunnetthi, L., Giovannoni, G., and Ramagopalan, S. V. (2010). An updated meta-analysis of risk of multiple sclerosis following infectious mononucleosis. *PLoS ONE*, *5*(9), 1–5. https://doi.org/10.1371/journal.pone.0012496

Harirchian, M. H., Fatehi, F., Sarraf, P., Honarvar, N. M., and Bitarafan, S. (2018). Worldwide prevalence of familial multiple sclerosis: A systematic review and meta-analysis. *Multiple Sclerosis and Related Disorders*, *20*(December 2017), 43–47. https://doi.org/10.1016/j.msard.2017.12.015

Hemond, C. C., and Bakshi, R. (2018). Magnetic resonance imaging in multiple sclerosis. *Cold Spring Harbor Perspectives in Medicine*, *8*(5), 1–22. https://doi.org/10.1101/cshperspect.a028969

Houtchens, M. K., Benedict, R. H. B., Killiany, R., Sharma, J., Jaisani, Z., Singh, B., Weinstock-Guttman, B., Guttmann, C. R. G., and Bakshi, R. (2007). Thalamic atrophy and cognition in multiple sclerosis. *Neurology*, *69*(12), 1213–1223. https://doi.org/10.1212/01.wnl.0000276992.17011.b5

Howard, J., Trevick, S., and Younger, D. S. (2016). Epidemiology of Multiple Sclerosis. *Neurologic Clinics*, *34*(4), 919–939. https://doi.org/10.1016/j.ncl.2016.06.016

Innocenti, G. M. (1994). Some new trends in the study of the corpus callosum. *Behavioural Brain Research*, *64*(1–2), 1–8. https://doi.org/10.1016/0166-4328(94)90113-9

Karakaş, P., Koç, Z., Koç, F., and Gülhal Bozkir, M. (2011). Morphometric MRI evaluation of corpus callosum and ventricles in normal adults. *Neurological Research*, *33*(10), 1044–1049. https://doi.org/10.1179/1743132811Y.0000000030

Karussis, D. (2014). The diagnosis of multiple sclerosis and the various related demyelinating syndromes: A critical review. *Journal of Autoimmunity*, *48–49*, 134–142. https://doi.org/10.1016/j.jaut.2014.01.022

Kearney, H., Cahalane, A. M., Killeen, R. P., and McGuigan, C. (2018). MRI and multiple sclerosis—the evolving role of MRI in the diagnosis and management of MS: a clinician's perspective. *Irish Journal of Medical Science*, *187*(2), 493–498. https://doi.org/10.1007/s11845-017-1691-z

Khasawneh, A., Garling, R., and Harris, C. (2018). Cerebrospinal fluid circulation: What do we know and how do we know it? *Brain Circulation*, *4*(1), 14. https://doi.org/10.4103/bc.bc_3_18

Kobelt, G., Thompson, A., Berg, J., Gannedahl, M., and Eriksson, J. (2017). New insights into the burden and costs of multiple sclerosis in Europe. *Multiple Sclerosis*, *23*(8), 1123–1136. https://doi.org/10.1177/1352458517694432

Korzh, V. (2018). Development of brain ventricular system. *Cellular and Molecular Life Sciences*, *75*(3), 375–383. https://doi.org/10.1007/s00018-017-2605-y

Kurtzke, J. F. (2013). Epidemiology in multiple sclerosis: a pilgrim's progress. *Brain*, *136*(9), 2904–2917. https://doi.org/10.1093/brain/awt220

Kwon, Y. H., Jang, S. H., and Yeo, S. S. (2014). Age-related changes of lateral ventricular width and periventricular white matter in the human brain: A diffusion tensor imaging study. *Neural Regeneration Research*, *9*(9), 986–989. https://doi.org/10.4103/1673-5374.133152

Laffon, M., Malandain, G., Joly, H., Cohen, M., and Lebrun, C. (2014). The HV3 Score: A New Simple Tool to Suspect Cognitive Impairment in Multiple Sclerosis in Clinical Practice. *Neurology and Therapy*, *3*(2), 113–122. https://doi.org/10.1007/s40120-014-0021-x

Larson, E. B., Burnison, D. S., and Brown, W. S. (2002). Callosal function in multiple sclerosis: Bimanual motor coordination. *Cortex*, *38*(2), 201–214. https://doi.org/10.1016/S0010-9452(08)70650-6

Lassmann, H. (2013). Pathology and disease mechanisms in different stages of multiple sclerosis. *Journal of the Neurological Sciences*, *333*(1–2), 1–4. https://doi.org/10.1016/j.jns.2013.05.010

Leray, E., Yaouanq, J., Le Page, E., Coustans, M., Laplaud, D., Oger, J., and Edan, G. (2010). Evidence for a two-stage disability progression in multiple sclerosis. *Brain*, *133*(7), 1900–1913. https://doi.org/10.1093/brain/awq076

Lublin, F. D., Reingold, S. C., Cohen, J. A., Cutter, G. R., Sørensen, P. S., Thompson, A. J., Wolinsky, J. S., Balcer, L. J., Banwell, B., Barkhof, F., Bebo, B., Calabresi, P. A., Clanet, M., Comi, G., Fox, R. J., Freedman, M. S., Goodman, A. D., Inglese, M., Kappos, L., … Polman, C. H. (2014). Defining the clinical course of multiple sclerosis: The 2013 revisions. *Neurology*, *83*(3), 278–286. https://doi.org/10.1212/WNL.0000000000000560

Lutz, T., Bellenberg, B., Schneider, R., Weiler, F., Köster, O., and Lukas, C. (2017). Central Atrophy Early in Multiple Sclerosis: Third Ventricle Volumetry versus Planimetry. *Journal of Neuroimaging*, *27*(3), 348–354. https://doi.org/10.1111/jon.12410

Maccabi, H., St, R. A., and Brak, B. (n.d.). *The Corpus Callosum: Normal Fetal Development as Shown by Transvaginal Sonography Gustavo 2 Haim Zakut1*. 1041–1043. www.ajronline.org

Mey, G. M., Mahajan, K. R., and DeSilva, T. M. (2022). Neurodegeneration in multiple sclerosis. *WIREs Mechanisms of Disease*, *July*, 1–25. https://doi.org/10.1002/wsbm.1583

Miller, D. H., Barkhof, F., Frank, J. A., Parker, G. J. M., and Thompson, A. J. (2002). Measurement of atrophy in multiple sclerosis: Pathological basis, methodological aspects and clinical relevance. *Brain*, *125*(8), 1676–1695. https://doi.org/10.1093/brain/awf177

Miller, D. H., Grossman, R. I., Reingold, S. C., and McFarland, H. F. (1998). The role of magnetic resonance techniques in understanding and managing multiple sclerosis. *Brain*, *121*(1), 3–24. https://doi.org/10.1093/brain/121.1.3

Moore, F. (2009). Incidental mri anomalies suggestive of multiple sclerosis: The radiologically isolated syndrome. *Neurology*, *73*(20), 1714. https://doi.org/10.1212/WNL.0b013e3181bd69a9

Mooshagian, E. (2008). Anatomy of the corpus callosum reveals its function. *Journal of*

Neuroscience, *28*(7), 1535–1536. https://doi.org/10.1523/JNEUROSCI.5426-07.2008

Morota, N., Watabe, T., Inukai, T., Hongo, K., and Nakagawa, H. (2000). Anatomical variants in the floor of the third ventricle: Implications for endoscopic third ventriculostomy. *Journal of Neurology Neurosurgery and Psychiatry*, *69*(4), 531–534. https://doi.org/10.1136/jnnp.69.4.531

Mortazavi, M. M., Adeeb, N., Griessenauer, C. J., Sheikh, H., Shahidi, S., Tubbs, R. I., and Tubbs, R. S. (2014). The ventricular system of the brain: A comprehensive review of its history, anatomy, histology, embryology, and surgical considerations. *Child's Nervous System*, *30*(1), 19–35. https://doi.org/10.1007/s00381-013-2321-3

Musiek, F. E. (1986). Neuroanatomy, neurophysiology, and central auditory assessment part III: Corpus callosum and efferent pathways. *Ear and Hearing*, *7*(6), 349–358. https://doi.org/10.1097/00003446-198612000-00001

Muti, E., Gruner, G., Dockery , P. (2016), Fitzgerald's Clinical Neuroanatomy and Neuroscience, International Editon, P. 19, ISBN: 978-0-7020-5832-5.

Orton, S. M., Herrera, B. M., Yee, I. M., Valdar, W., Ramagopalan, S. V., Sadovnick, A. D., and Ebers, G. C. (2006). Sex ratio of multiple sclerosis in Canada: a longitudinal study. *Lancet Neurology*, *5*(11), 932–936. https://doi.org/10.1016/S1474-4422(06)70581-6

Pakpoor, J., Disanto, G., Gerber, J. E., Dobson, R., Meier, U. C., Giovannoni, G., and Ramagopalan, S. V. (2013). The risk of developing multiple sclerosis in individuals seronegative for Epstein-Barr virus: A meta-analysis. *Multiple Sclerosis Journal*, *19*(2), 162–166. https://doi.org/10.1177/1352458512449682

Palacios, N., Alonso, A., BrØnnum-Hansen, H., and Ascherio, A. (2011). Smoking and Increased Risk of Multiple Sclerosis: Parallel Trends in the Sex Ratio Reinforce the Evidence. *Annals of Epidemiology*, *21*(7), 536–542. https://doi.org/10.1016/j.annepidem.2011.03.001

Pashaj, S., Merz, E., and Wellek, S. (2013). Biometry of the fetal corpus callosum by three-dimensional ultrasound. *Ultrasound in Obstetrics and Gynecology*, *42*(6), 691–698. https://doi.org/10.1002/uog.12501

Patnaik, P., Singh, V., Singh, D., and Singh, S. (2015). Gender Related Differences in Third Ventricle Parameters with Correlation to Cerebrum Size-A Study on Head CT Scans. *International Journal of Health Sciences & Research (Www.Ijhsr.Org)*, *5*(November), 11. www.ijhsr.org

Patra, A., Kumar, S. R., Tubbs, R. S., Nandolia, K., and Asghar, A. (2022). The Morphology and Morphometry of the Human Interthalamic Adhesion Using Cadaveric Brains and Magnetic Resonance Images and Their Clinical Significance. *Turkish Neurosurgery*, *32*(6), 960–967. https://doi.org/10.5137/1019-5149.JTN.36551-21.2

Paul, L. K. (2011). Developmental malformation of the corpus callosum: A review of typical callosal development and examples of developmental disorders with callosal involvement. *Journal of Neurodevelopmental Disorders*, *3*(1), 3–27. https://doi.org/10.1007/s11689-010-9059-y

Pérez-Martín, M. Y., González-Platas, M., Jiménez-Sosa, A., Plata-Bello, J., and López-Segura, A. (2020). Normative Data of the Corpus Callosum Index and Discriminant Validity in Patients with Multiple Sclerosis. *J Neurol Neurosci*, *11*(4), 322. https://doi.org/10.36648/2171-6625.11.1.322

Polman, C. H., Reingold, S. C., Banwell, B., Clanet, M., Cohen, J. A., Filippi, M., Fujihara, K., Havrdova, E., Hutchinson, M., Kappos, L., Lublin, F. D., Montalban, X., O'Connor, P., Sandberg-Wollheim, M., Thompson, A. J., Waubant, E., Weinshenker, B., and Wolinsky, J. S. (2011). Diagnostic criteria for multiple sclerosis: 2010 Revisions to the McDonald criteria. *Annals of Neurology*, *69*(2), 292–302.

https://doi.org/10.1002/ana.22366

Preziosa, P., Rocca, M. A., Pagani, E., Stromillo, M. L., Enzinger, C., Gallo, A., Hulst, H. E., Atzori, M., Pareto, D., Riccitelli, G. C., Copetti, M., De Stefano, N., Fazekas, F., Bisecco, A., Barkhof, F., Yousry, T. A., Arévalo, M. J., and Filippi, M. (2016). Structural MRI correlates of cognitive impairment in patients with multiple sclerosis: A Multicenter Study Structural MRI Correlates of Cognitive Impairment in Patients With Multiple Sclerosis: A Multicenter Study Cognitive Impairment and Brain Damage in . *Human Brain Mapping*, *37*(4), 1627–1644. https://doi.org/10.1002/hbm.23125

Raybaud, C. (2010). The corpus callosum, the other great forebrain commissures, and the septum pellucidum: Anatomy, development, and malformation. *Neuroradiology*, *52*(6), 447–477. https://doi.org/10.1007/s00234-010-0696-3

Rhoton, A. L. (2007). The cerebrum. *Neurosurgery*, *61*(1 SUPPL.), 37–119. https://doi.org/10.1227/01.NEU.0000255490.88321.CE

Riccitelli, G., Rocca, M. A., Pagani, E., Rodegher, M. E., Rossi, P., Falini, A., Comi, G., and Filippi, M. (2011). Cognitive impairment in multiple sclerosis is associated to different patterns of gray matter atrophy according to clinical phenotype. *Human Brain Mapping*, *32*(10), 1535–1543. https://doi.org/10.1002/hbm.21125

Ristori, G., Cannoni, S., Stazi, M. A., Vanacore, N., Cotichini, R., Alfò, M., Pugliatti, M., Sotgiu, S., Solaro, C., Bomprezzi, R., Di Giovanni, S., Talamanca, L. F., Nisticò, L., Fagnani, C., Neale, M. C., Cascino, I., Giorgi, G., Battaglia, M. A., Buttinelli, C., … Salvetti, M. (2006). Multiple sclerosis in twins from continental Italy and Sardinia: A nationwide study. *Annals of Neurology*, *59*(1), 27–34. https://doi.org/10.1002/ana.20683

Roosendaal, S. D., Bendfeldt, K., Vrenken, H., Polman, C. H., Borgwardt, S., Radue, E. W., Kappos, L., Pelletier, D., Hauser, S. L., Matthews, P. M., Barkhof, F., and Geurts, J. J. G. (2011). Grey matter volume in a large cohort of MS patients: Relation to MRI parameters and disability. *Multiple Sclerosis Journal*, *17*(9), 1098–1106. https://doi.org/10.1177/1352458511404916

Ryberg, C., Stegmann, M. B., Sjöstrand, K., Rostrup, E., Fazekas, F., Barkhof, F., and Waldemar, G. (2006). Corpus Callosum Partitioning Schemes and Their Effect on Callosal Morphometry. *Neuroepidemiology*, *23*(6), 5–5. http://orbit.dtu.dk/app?cdis=attachment;+filename=%22imm4410.pdf%22&ctyp=&downloadOptionName=URL&service=download_records&url=http://urbit.cvt.dk/cgi-bin/urbit_fulltext/191594/1/1/c61c37fd19b2d339a09804f2ff227c7a

Sakai, T., Mikami, A., Suzuki, J., Miyabe-Nishiwaki, T., Matsui, M., Tomonaga, M., Hamada, Y., Matsuzawa, T., Okano, H., and Oishi, K. (2017). Developmental trajectory of the corpus callosum from infancy to the juvenile stage: Comparative MRI between chimpanzees and humans. *PLoS ONE*, *12*(6), 1–22. https://doi.org/10.1371/journal.pone.0179624

Schiller, F. (1997). The cerebral ventricles from soul to sink. *Archives of Neurology*, *54*(9), 1158–1162. https://doi.org/10.1001/archneur.1997.00550210086018

Schminke, U., Lorenz, L., Kirsch, M., Sarnowski, B. Von, Khaw, A. V, Kessler, C., and Dressel, A. (2009). *Diameter Assessment of the Third Ventricle with Transcranial Sonography in Patients with Multiple Sclerosis*. 53–57. https://doi.org/10.1111/j.1552-6569.2008.00321.x

Schuenke, M. (2016), ThIeme Atlas of Anatomy, ThIeme Medıcal Publıshers, New Your, P. 303-306. ISBN: 978-1-62623-120-7.

Shiino, A., Chen, Y. W., Tanigaki, K., Yamada, A., Vigers, P., Watanabe, T., Tooyama, I., and Akiguchi, I. (2017). Sex-related difference in human white matter volumes studied: Inspection of the corpus callosum and other white matter by VBM. *Scientific Reports*,

7(January), 3–9. https://doi.org/10.1038/srep39818

Sintzel, M. B., Rametta, M., and Reder, A. T. (2018). Vitamin D and Multiple Sclerosis: A Comprehensive Review. *Neurology and Therapy*, *7*(1), 59–85. https://doi.org/10.1007/s40120-017-0086-4

Stratchko, L., Filatova, I., Agarwal, A., and Kanekar, S. (2016). The Ventricular System of the Brain: Anatomy and Normal Variations. *Seminars in Ultrasound, CT and MRI*, *37*(2), 72–83. https://doi.org/10.1053/j.sult.2016.01.004

Suganthy, J., Raghuram, L., Antonisamy, B., Vettivel, S., Madhavi, C., and Koshi, R. (2003). Gender- and age-related differences in the morphology of the corpus callosum. *Clinical Anatomy*, *16*(5), 396–403. https://doi.org/10.1002/ca.10161

Sullivan, E. V., Rosenbloom, M. J., Desmond, J. E., and Pfefferbaum, A. (2001). Sex differences in corpus callosum size: Relationship to age and intracranial size. *Neurobiology of Aging*, *22*(4), 603–611. https://doi.org/10.1016/S0197-4580(01)00232-9

Tanaka-Arakawa, M. M., Matsui, M., Tanaka, C., Uematsu, A., Uda, S., Miura, K., Sakai, T., and Noguchi, K. (2015). Developmental changes in the corpus callosum from infancy to early adulthood: A structural magnetic resonance imaging study. *PLoS ONE*, *10*(3), 1–13. https://doi.org/10.1371/journal.pone.0118760

Thompson, A. J., Banwell, B. L., Barkhof, F., Carroll, W. M., Coetzee, T., Comi, G., Correale, J., Fazekas, F., Filippi, M., Freedman, M. S., Fujihara, K., Galetta, S. L., Hartung, H. P., Kappos, L., Lublin, F. D., Marrie, R. A., Miller, A. E., Miller, D. H., Montalban, X., … Cohen, J. A. (2018). Diagnosis of multiple sclerosis: 2017 revisions of the McDonald criteria. *The Lancet Neurology*, *17*(2), 162–173. https://doi.org/10.1016/S1474-4422(17)30470-2

Tracy, S. I., Kakalacheva, K., Lünemann, J. D., Luzuriaga, K., Middeldorp, J., and Thorley-Lawson, D. A. (2012). Persistence of Epstein-Barr Virus in Self-Reactive Memory B Cells. *Journal of Virology*, *86*(22), 12330–12340. https://doi.org/10.1128/jvi.01699-12

Trapp, B. D., Peterson, J., Ransohoff, R. M., Rudick, R., Mörk, S., and Bö, L. (1998). Axonal Transection in the Lesions of Multiple Sclerosis. *New England Journal of Medicine*, *338*(5), 278–285. https://doi.org/10.1056/nejm199801293380502

Travers, B. S., and Tsang, B. K. (2022). *Multiple sclerosis*. *51*(4), 199–206.

Tsutsumi, S., Ishii, H., Ono, H., and Yasumoto, Y. (2018). The third ventricle roof: an anatomical study using constructive interference in steady-state magnetic resonance imaging. *Surgical and Radiologic Anatomy*, *40*(2), 123–128. https://doi.org/10.1007/s00276-017-1905-0

Tubbs, R. S., Loukas, M., Shoja, M. M., Shokouhi, G., and Oakes, W. J. (2008). François Magendie (1783-1855) and his contributions to the foundations of neuroscience and neurosurgery. *Journal of Neurosurgery*, *108*(5), 1038–1042. https://doi.org/10.3171/JNS/2008/108/5/1038

Tubbs, R. S., Oakes, P., Maran, I. S., Salib, C., and Loukas, M. (2014). The foramen of Monro: a review of its anatomy, history, pathology, and surgery. *Child's Nervous System*, *30*(10), 1645–1649. https://doi.org/10.1007/s00381-014-2512-6

Tuncer, C. M., Hatipoğlu, E. S., and Özateş, M. (2005). Sexual dimorphism and handedness in the human corpus callosum based on magnetic resonance imaging. *Surgical and Radiologic Anatomy*, *27*(3), 254–259. https://doi.org/10.1007/s00276-004-0308-1

Vanderah, T.W., Gould , D.J. (2016), Nolte's The Human Brain An Introducton To İts Functional Anatomy, P: 13, Elsevier Copy Right. İSBN: 987-1-4557-2859-6.

Van der Knaap, L. J., and van der Ham, I. J. M. (2011). How does the corpus callosum mediate interhemispheric transfer? A review. *Behavioural Brain Research*, *223*(1), 211–221.

https://doi.org/10.1016/j.bbr.2011.04.018

Van Schependom, J., Jain, S., Cambron, M., Vanbinst, A. M., De Mey, J., Smeets, D., and Nagels, G. (2016). Reliability of measuring regional callosal atrophy in neurodegenerative diseases. *NeuroImage: Clinical*, *12*, 825–831. https://doi.org/10.1016/j.nicl.2016.10.012

Voskuhl, R. R., Patel, K., Paul, F., Gold, S. M., Scheel, M., Kuchling, J., Cooper, G., Asseyer, S., Chien, C., Brandt, A. U., Meyer, C. E., and MacKenzie-Graham, A. (2020). Sex differences in brain atrophy in multiple sclerosis. *Biology of Sex Differences*, *11*(1), 1–10. https://doi.org/10.1186/s13293-020-00326-3

Wang, S. Sen, Zheng, H. P., Zhang, F. H., and Wang, R. M. (2011). The microanatomical structure of the cistern of the lamina terminalis. *Journal of Clinical Neuroscience*, *18*(2), 253–259. https://doi.org/10.1016/j.jocn.2010.03.065

Wattjes, M. P., Rovira, À., Miller, D., Yousry, T. A., Sormani, M. P., De Stefano, N., Tintoré, M., Auger, C., Tur, C., Filippi, M., Rocca, M. A., Fazekas, F., Kappos, L., Polman, C., Barkhof, F., and Montalban, X. (2015). Evidence-based guidelines: MAGNIMS consensus guidelines on the use of MRI in multiple sclerosis - Establishing disease prognosis and monitoring patients. *Nature Reviews Neurology*, *11*(10), 597–606. https://doi.org/10.1038/nrneurol.2015.157

Witelson, S. F. (1989). Hand and sex differences in the isthmus and genu of the human corpus callosum: A postmortem morphological study. *Brain*, *112*(3), 799–835. https://doi.org/10.1093/brain/112.3.799

Zhuravlova, I., and Kornieieva, M. (2021). Anatomic Variability of the Morphometric Parameters of the Third Ventricle of the Brain and Its Relations to the Shape of the Skull. *Journal of Neurological Surgery, Part B: Skull Base*, *82*, E315–E320. https://doi.org/10.1055/s-0040-1701527

Zohdi, A., and Elkheshin, S. (2012). Endoscopic anatomy of the velum interpositum: A sequential descriptive anatomical study. *Asian Journal of Neurosurgery*, *7*(01), 12–16. https://doi.org/10.4103/1793-5482.95689

T.C.
ONDOKUZ MAYIS ÜNİVERSİTESİ
KLİNİK ARAŞTIRMALAR ETİK KURULU

Sayı: B.30.2.ODM.0.20.08/496-569 04.08.2020

Sayın Doç.Dr.Mennan Ece PİRZİRENLİ

Etik Kurulumuza sunmuş olduğunuz **Multiple Skleroz Hastalarında Üçüncü Ventrikül ve Corpus Callosum Anatomisinin Morfometrik Analizi:Manyetik Rezonans Görüntüleme Çalışması** başlıklı OMÜ KAEK 2020/481 Karar nolu Radyoloji çalışması+ Dosya taraması nitelikli araştırma projeniz amaç, gerekçe, yaklaşım ve yöntemle ilgili açıklamaları, Klinik Araştırmalar Etik kurulu yönergesine göre 23.07.2020 tarihli Etik Kurulumuzda incelenmiş etik açıdan uygun bulunmuştur. Ancak araştırma bütçesinin maddi desteği henüz sağlanamadığından projeye bütçe desteği sağlanıp, tarafımıza bildirilmesinden sonra başlanmasına oy birliği ile karar verilmiştir

Bilgilerinize arz/rica ederim.

Ondokuz mayıs Üniversitesi Klinik Araştırmalar Etik Kurulu Tel (0362)3121919/2782 -4576007 Omutaek@gmail.com
Eski Diş Hekimliği Fakültesi 2.Kat Atakum/SAMSUN

CURRICULUM VITEA

Hussam Alabdullah

ORCID: 0009-0004-2652-6075

Publications :

- A research entitled (Anatomical Evaluation of the Corpus Callosum in Multiple Sclerosis Patients Using MRI) was published in (Journal of Population Therapeutics and Clinical Pharmacology).
- A research entitled (Morphometric Analysis of the Third Ventricle in Multiple Sclerosis patients Using MRI) was accepted in (History of Medicine) journal.

Education and Qualifications:

- Bachelor's degree in Medicine, University of Aleppo, Faculty of Medicine 2001-2007.
- General Surgery Resident at Aleppo University Hospital 2007-2012.
- Certificate of the Arab Board for Health Specializations, Surgery 2016.
- Full Turkish Equivalency of Medical degree after passing STS exam and completion of clinical training at Mustafa Kemal University, Hatay, TÜRKİYE, 2021.
- Full Membership of the Royal College of Surgeons, MRCS. Edinburgh, UK, 2022.
- Ph.D. student at Ondokuz Mayıs University, Faculty of Medicine, Department of Anatomy, Samsun, TÜRKİYE.
- Faculty member and trainer at (Surgery in Hostile Environment course) Provided by Dr. David Nott Foundation.

Practical Experience:

Worked as a specialist general surgeon in:

- 2020- till now: Çobanbey Hospital in north Syria (related to the Turkish red crescent in north Syria).
- 2015-2019: MSF Alsalamah Hospital in north Syria (Doctors without Borders, Spanish branch).
- 2013-2014: M1 Field Hospital, Aleppo City.